Resource Allocation for D2D Communication Underlaid Cellular Networks Using Graph-based Approach

Tuong Duc Hoang, *Student Member, IEEE,* Long Bao Le, *Senior Member, IEEE,* and Tho Le-Ngoc, *Fellow, IEEE*

***Abstract*—In this paper, we study the non-orthogonal dynamic spectrum sharing for device-to-device (D2D) communications in the D2D underlaid cellular network. Our design aims to maximize the weighted system sum-rate under the constraints that (i) each cellular or active D2D link is assigned one subband and (ii) the required minimum rates for cellular and active D2D links are guaranteed. To solve this problem, we first characterize the optimal power allocation solution for a given subband assignment. Based on this result, we formulate the subband assignment problem by using the graph-based approach, in which each link corresponds to a vertex and each subband assignment is represented by a hyper-edge. We then propose an Iterative Rounding algorithm and an optimal Branch-and-Bound (BnB) algorithm to solve the resulting graph-based problem. We prove that the Iterative Rounding algorithm achieves at least 1/2 of the optimal weighted sum-rate. Extensive numerical studies illustrate that the proposed Iterative Rounding algorithm significantly outperforms conventional spectrum sharing algorithms and attains almost the same system sum-rate as the optimal BnB algorithm.**

***Index Terms*—Device-to-device communication, cellular networks, resource allocation, subband assignment, power allocation.**

I. Introduction

The fast growth of mobile traffic has motivated the development of enabling technologies for significant network capacity enhancement in future wireless networks [1]. Device-to-device communications has been proposed as a mean to improve the system spectral and energy-efficiency and reduce traffic load in the core network [2]–[4]. Specifically, in the dense networks, D2D communications can improve the system spectral efficiency significantly since spatial spectrum reuse is exploited effectively through enabling short-range D2D communication links. Efficient radio resource management for D2D communications is essential to realize these benefits.

In general, spectrum assignment for cellular and D2D links can be performed in the orthogonal or non-orthogonal manner [5]. Moreover, non-orthogonal resource allocation for D2D and cellular links can be divided into three scenarios as described in the following.

Manuscript received June 26, 2015; revised December 08, 2015 and May 15, 2016; accepted July 23, 2016.

T. D. Hoang and L. B. Le are with INRS-EMT, Université du Québec, Montréal, Québec, Canada. Emails: {tuong.hoang,long.le}@emt.inrs.ca.

T. Le-Ngoc is with Department of Electrical and Computer Engineering, McGill University, Montréal, Québec, Canada. Emails: tho.le-ngoc@mcgill.ca

Scenario I: Each active (admitted) D2D link is assigned one subband and each subband is exploited by at most one D2D link. This scenario allows us to design efficient and low-complexity algorithms, which can be used to address the design in more general settings. This scenario is especially beneficial for the dense deployment of D2D communications.

Scenario II: Each active (admitted) D2D link can be assigned multiple subbands and each subband is exploited by at most one D2D link. This scenario requires more complicated resource allocation design compared to scenario I. This is because beside the design issues of scenario I, scenario II requires to determine the number of subbands allocated to each D2D link.

Scenario III: Each active (admitted) D2D link can be assigned multiple subbands and each subband can be exploited by multiple D2D links. Resource allocation for this scenario is certainly very challenging. In fact, even if the subband assignment solution can be determined, the power allocation problem is still strongly NP-Hard [6]; therefore, only heuristic algorithms can be developed to obtain a feasible solution with practically affordable computation complexity. Furthermore, to solve the resource allocation in this scenario, the channel state information (CSI) of the interfering channels among D2D links over all subbands must be available. Estimation of such CSI may not be feasible in many practical D2D applications, especially in the dense D2D communications setting, due to the large CSI estimation and signaling overhead.

Due to the potential benefits of studying scenario I, many existing works focus on designing efficient resource allocation algorithms for this scenario [7]–[14]. Early works consider simple network settings such as the system with only one cellular link and one D2D link [7]. Moreover, most existing resource allocation designs assume that channel allocations for cellular links have been predetermined [7]–[22]. From the admission control perspective, the current literature either ignores the link selection issue or proposes only greedy link selection algorithms [10], [13], [17], [21]. Generally, D2D communications can be assisted and controlled by the cellular base-station (BS) [5] through which optimization of the subband assignment, power allocation, and link selection for both cellular and D2D links would lead to the best system performance.

Solving this joint design problem for any aforementioned scenarios requires us to deal with the nonlinear power allocation and optimization of integer variables related to the subband assignments and link selection. Even for a given power

TABLE I
SUMMARY OF RELATED WORKS AND OUR CURRENT WORK

Ref.	Scenario	Approach	Objective	QoS	Model	SA for cellular links	Link selection	Multi-D2D and cellular links	Theoretical performance analysis	Optimal solution
[7]	I	Optimization	Sum-rate	No	PA	No	No	No	Yes	Yes
[8]	I	Optimization	Sum-rate	Yes	PA	No	No	No	Yes	No
[9]	I	Optimization	Energy efficiency	Yes	PA	No	No	No	No	No
[10]	I	Optimization	Sum-rate	Yes	PA	No	Yes	No	Yes	Yes
[11]	I	Optimization	Sum-rate	Yes	SA, PA	No	No	Yes	Yes	Yes
[12]	I	Optimization	Sum-rate	Yes	SA, PA	No	No	Yes	No	No
[13]	I	Optimization	Weighted sum-rate	Yes	SA, PA	Yes	Yes	No	No	No
[14]	I	Game theory	Sum-rate	Yes	PA, SA	No	No	Yes	No	No
[15]	I	Optimization	Sum-rate	Yes	PA, SA	No	No	No	No	No
[16]	III	Optimization	Sum-rate	No	PA	No	No	No	No	No
[17]	III	Dynamic programming	Number of required subchannels	Yes	No	No	Yes	No	No	No
[18]	III	Dynamic programming	Sum-rate	No	SA, PA	No	No	Yes	No	No
[19]	III	Graph based	Sum utility	Yes	SA, PA	No	No	Yes	No	No
[20]	III	Optimization and game theory	Sum rate	Yes	PA	No	No	Yes	No	No
[21]	III	Optimization	Sum-rate	No	SA, PA	No	Yes	No	No	No
[22]	III	Graph based	Sum-rate	No	SA, PA	No	Yes	No	No	No
[23]	III	Graph based	Sum-rate	No	NA	Yes	No	Yes	No	No
[24]	I	Game theory	Sum-rate	Yes	PA, SA	No	No	Yes	No	No
[25], [26]	III	Game theory	Sum-rate	Yes	PA, SA	No	No	Yes	No	No
[27]	II	Game theory	Energy-efficient	Yes	PA, SA	No	No	Yes	No	No
[28]	II	Game theory	Sum-rate	Yes	PA, SA	No	No	Yes	No	No
[29]	III	Game theory	Sum utility	Yes	PA, SA	No	No	Yes	No	No
Our work	I, II	Graph based and optimization	Weighted sum-rate	Yes	SA, PA	Yes	Yes	Yes	Yes	Yes

allocation and link selection solution, we still need to tackle an integer subband assignment problem, which is NP-Hard in general. Therefore, it is very challenging to tackle this joint design problem even for scenario I. Moreover, development of an efficient and low-complexity resource allocation algorithm is of great interest for practical implementation. The current work focuses on resource allocation design for scenarios I and II and we reserve the study of scenario III for our future works.

A. Related Works

Resource allocation design for the setting in which D2D and cellular links share a single channel is investigated in [7]–[10], [16]. In particular, the authors of [7] consider the power allocation and mode selection problem to maximize the sum-rate where they study the power allocation problem for each mode where there are only one cellular link and one D2D link. Joint power and rate control of D2D and cellular links is studied in [8], and the mode switching problem for D2D communication is investigated in [9]. Both works [8] and [9], however, consider the system with one D2D link and one cellular link. In [10], the power control design is pursued to optimize the spectrum efficiency of D2D links in vehicular systems while the joint admission control, mode selection, and power control problem is studied for a general D2D communication system in [16]. Both works [10] and [16] consider the systems with multiple cellular and D2D links and a single channel.

In general, joint optimization of subband and power allocation is required for efficient resource utilization in multi-channel wireless systems. The setting with multiple D2D and cellular links sharing multiple channels is considered in several recent works [11]–[15]. In [11], the system sum-rate optimization for D2D and cellular links is considered. Nonetheless, the authors assume that each cellular link has been pre-allocated one subband and the work aims at optimizing the matching of each D2D link with one cellular link so that the sum rate is maximized. The joint D2D mode selection and resource allocation framework is proposed in [12] where each D2D link can either reuse the resource of cellular links or exploit the dedicated resource assuming that the resource allocation for cellular links is pre-determined. Resource allocation for D2D communication is investigated in [13] where the heuristic matching design between D2D and cellular links based on their relative distance is adopted. Moreover, the stable marriage matching algorithms are adopted in [14], [15] to determine the efficient matching between cellular and D2D links. Although all these existing works focus on scenario I mentioned above, link selection is not studied, these works assume that the resource allocations of the cellular links are pre-determined.

Resource allocation designs, which allow multiple D2D links to reuse the same resource, are studied in several recent papers [17]–[23], [30], [31]. In particular, the works in [17] and [18] employ the dynamic programming approach to solve the resource allocation for the D2D underlaying cellular

network. The joint subchannel and power allocation design using an interference-graph method is conducted in [23], a semi-distributed resource allocation algorithm is proposed in [19], and the iterative algorithms are developed in [30], [31]. However, the authors propose to share the downlink cellular resources with D2D links, which is not recommended in the LTE-A standard. In [20], the authors propose a joint spectrum and power allocation algorithm for the D2D underlaying cellular system assuming that the power of each D2D link is fixed and the interference from cellular links to D2D links is negligible. Moreover, in [21], a two-step resource allocation algorithm is proposed where greedy subband assignment is performed in the second step after the power allocation in the first step. Finally, in [22] the graph coloring algorithm is proposed to match cellular resources with one or two D2D links; nevertheless, the power allocation is not studied. For most aforementioned works, the channel assignments for cellular links are assumed to be pre-determined, only heuristic algorithms are proposed, and link selection for D2D links is not investigated.

Game theory has also been employed for D2D resource allocation design in several existing works [24]–[29]. Auction based resource allocation for D2D communications is studied in [24]. The two-stage Stackelberg game is employed to engineer the resource allocation in [25] where the cellular BS is the leader and D2D links are the followers. Non-cooperative game formulation is adopted to design the resource allocation for D2D links in [26], and the coalitional game approach is employed to solve the joint mode selection and resource allocation in [28]. For the game theory approach adopted in [24]–[29], D2D and cellular links usually act as the players and the obtained stable solution could be satisfactory for all users but it may not be necessarily the most efficient solution. Moreover, these works do not consider link selection for D2D links and subband assignment optimization for cellular links.

We summarize these related works and their characteristics in Table I where PA and SA stand for power allocation and subband allocation, respectively. It can be observed that none of these existing works addresses all following design aspects: consideration of a general setting with multiple cellular and D2D links, joint subband allocation optimization for cellular and D2D links, D2D link selection, QoS guarantees for both cellular and D2D links, and theoretical performance analysis of developed sub-optimal algorithms.

B. Contributions and Novelty of the Current Work

This paper focuses on the radio resource allocation for D2D communications in cellular networks for the first scenario and the developed algorithm for scenario I is employed to tackle the resource allocation for scenario II. Specifically, our work makes the following contributions.

- We formulate the resource allocation problem for joint D2D link selection, subband assignment, and power control that aims at maximizing the weighted sum-rate while guaranteeing the minimum rate requirements of individual cellular and active (selected) D2D links. The D2D link selection is indeed embedded into the considered joint optimization problem in our design. Moreover, to solve this problem, we first derive the optimal power allocation for a given subband assignment for one pair of cellular and D2D links, which enables us to determine the contribution of each subband assignment to the optimization objective. Based on this result, we transform the original resource allocation problem into the subband assignment problem.
- We formulate the subband assignment problem by employing the graph-based approach. Since each link can exploit a subband orthogonally or non-orthogonally, we introduce the concept of virtual cellular and D2D links to capture all possible types of subband assignments. We then formulate a graph-based problem where each link/subband and subband assignment correspond to one vertex and one hyper-edge in the underlying graph, respectively. This problem belongs to the family of three-dimensional matching problems, which are generally NP-Hard.
- We develop a novel Iterative Rounding algorithm to solve the subband assignment problem based on the combination of linear programming and efficient rounding techniques. Specifically, in each iteration we solve a relaxed version of the subband assignment problem for unallocated subbands and network links. Then, we develop a sophisticated mechanism to arrange fractional-weight edges of the underlying graph in an appropriate order and employ the *Local Ratio Method* [32] to determine some subband assignments. Moreover, the unassigned subbands and network links are used to form the network graph based on which we can decide further subband assignments in the next iteration by using the same procedure. We prove that the weighted sum-rate achieved by this Iterative Rounding algorithm is at least half of the optimal weighted sum-rate. In addition, we present an optimal Branch and Bound (BnB) algorithm, which has significantly lower computational complexity compared to the optimal exhaustive search algorithm.
- Numerical results demonstrate that the Iterative Rounding algorithm achieves almost the same sum-rate as that attained by the optimal BnB algorithm. In addition, these two algorithms result in up to 40% sum-rate gain compared to the conventional algorithms in [13] and [14]. Moreover, numerical results also confirm that in the dense D2D communications scenario, resource allocation design under scenario I can achieve reasonably good performance. Finally, we show that by using the Iterative Rounding algorithm in the two-step design approach to address scenario II, we can achieve dramatically higher sum-rate than those due to the conventional algorithms in [27], [28].

The remaining of this paper is organized as follows. In Section II, we describe the system model and problem formulation. The optimal power allocation is described in Section III, followed by the description of subband assignment algorithms in Section IV. Discussions of algorithm complexity, signaling, and further extensions are given in Section V. In Section VI,

we present the numerical results, and Section VII concludes the paper.

II. System Model and Problem Formulation

A. System Model

We consider the spectrum sharing problem among multiple D2D and cellular links in the uplink direction. Let $\mathcal{N} = \{1, \cdots, N\}$ with size $|\mathcal{N}| = N$ be the set of subbands in the system.[1] We denote $\mathcal{K}_c = \{1, \cdots, K_c\}$ as the set of cellular links, $\mathcal{K}_d = \{K_c + 1, \cdots, K_c + K_d\}$ as the set of D2D links, and $\mathcal{K} = \mathcal{K}_c \cup \mathcal{K}_d$ as the set of all communications links with size $|\mathcal{K}| = K_c + K_d = K$. We assume that each subband can be allocated to at most one cellular and one D2D link, which means that cellular and D2D links utilize available subbands orthogonally within its tier.

Let $h_{kl}^{[n]}$ be the channel gain from the transmitter of link l to the receiver of link k on subband n. We denote $P_k^{\max}$ as the maximum transmit power of link $k \in \mathcal{K}$. In addition, we denote the power vectors on subband n and all the subbands as $\mathbf{p}^{[n]} = [p_1^{[n]}, \cdots, p_K^{[n]}]^T$, and $\mathbf{p} = \text{vec}[\mathbf{p}^{[1]}, \cdots, \mathbf{p}^{[N]}]$, respectively. For clarity, we will also use $p_{Ck}^{[n]}$ and $p_{Dl}^{[n]}$ to explicitly denote the powers of cellular link k and D2D link l on subband n, respectively. To represent assignment decision of subband n to link $k \in \mathcal{K}$, we define a binary variable $\rho_k^{[n]}$ where $\rho_k^{[n]} = 1$ if the subband n is assigned to link $k \in \mathcal{K}$, and $\rho_k^{[n]} = 0$, otherwise. We also define the subband assignment vectors $\boldsymbol{\rho}^{[n]} = [\rho_1^{[n]}, \cdots, \rho_K^{[n]}]^T$ and $\boldsymbol{\rho} = \text{vec}[\boldsymbol{\rho}^{[1]}, \cdots, \boldsymbol{\rho}^{[N]}]$. For convenience, we adopt the following notations: $\mathcal{K}_k \equiv \mathcal{K}_c$ if $k \in \mathcal{K}_c$ and $\mathcal{K}_k \equiv \mathcal{K}_d$ if $k \in \mathcal{K}_d$.

The signal to interference plus noise ratio (SINR) achieved by link $k \in \mathcal{K}$ on subband n can be expressed as

$$\Gamma_k^{[n]}(\mathbf{p}^{[n]}, \boldsymbol{\rho}^{[n]}) = \frac{\rho_k^{[n]} p_k^{[n]} h_{kk}^{[n]}}{\sigma_k^{[n]} + \sum_{l \in \mathcal{K} \backslash \mathcal{K}_k} \rho_l^{[n]} p_l^{[n]} h_{kl}^{[n]}}, \tag{1}$$

where $\sigma_k^{[n]}$ denotes the noise power for link k on subband n, and $\sum_{l \in \mathcal{K} \backslash \mathcal{K}_k} \rho_l^{[n]} p_l^{[n]} h_{kl}^{[n]}$ is the interference due to other links in the $\mathcal{K} \backslash \mathcal{K}_k$ set. The achievable rates of link $k \in \mathcal{K}$ on subband n and all the subbands can be expressed as

$$r_k^{[n]}(\mathbf{p}^{[n]}, \boldsymbol{\rho}^{[n]}) = \log_2 \left(1 + \Gamma_k^{[n]}(\mathbf{p}^{[n]}, \boldsymbol{\rho}^{[n]})\right), \tag{2}$$

$$r_k(\mathbf{p}, \boldsymbol{\rho}) = \sum_{n \in \mathcal{N}} r_k^{[n]}(\mathbf{p}^{[n]}, \boldsymbol{\rho}^{[n]}), \tag{3}$$

where the rate is calculated in b/s/Hz, which is normalized by the bandwidth of one subband.

B. Problem Formulation

We assume that each cellular link or active D2D link is allocated one subband, which is suitable for uplink communications [33].[2] Our design objective is to maximize the weighted sum-rate of all selected D2D links and cellular links while satisfying the minimum required rates of cellular links and active D2D links. Specifically, the QoS requirements of cellular links are expressed as[3]

$$r_k(\mathbf{p}, \boldsymbol{\rho}) \geq R_k^{\min} \ \forall k \in \mathcal{K}_c. \tag{4}$$

In addition, the minimum rate requirement of an D2D link when it is selected is described as

$$r_k(\mathbf{p}, \boldsymbol{\rho}) \geq \mathbf{I}\{\sum_{n \in \mathcal{N}} \rho_k^{[n]} = 1\} R_k^{\min} \ \forall k \in \mathcal{K}_d, \tag{5}$$

where $\mathbf{I}\{A\}$ denotes the indicator function, which equals to 1 if A is true and equals 0, otherwise. Here, we have $\sum_{n \in \mathcal{N}} \rho_k^{[n]} = 1$ for each selected D2D link k, which is assigned exactly one subband. The power constraints of all the links are given as

$$\sum_{n \in \mathcal{N}} p_k^{[n]} \leq P_k^{\max} \ \forall k \in \mathcal{K}. \tag{6}$$

Moreover, we assume that each subband can be allocated to only one cellular link and one D2D link, which is captured by the following constraints

$$\sum_{k \in \mathcal{K}_c} \rho_k^{[n]} \leq 1 \ \forall n \in \mathcal{N} \tag{7}$$

$$\sum_{k \in \mathcal{K}_d} \rho_k^{[n]} \leq 1 \ \ \forall n \in \mathcal{N}. \tag{8}$$

In addition, each cellular link is assigned one subband and each D2D link can use one subband, which are captured by the following subband assignment constraints

$$\sum_{n \in \mathcal{N}} \rho_k^{[n]} = 1 \ \forall k \in \mathcal{K}_c \tag{9}$$

$$\sum_{n \in \mathcal{N}} \rho_k^{[n]} \leq 1 \ \forall k \in \mathcal{K}_d \tag{10}$$

$$\rho_k^{[n]} \in \{0, 1\} \ \forall k \in \mathcal{K} \ \forall n \in \mathcal{N}. \tag{11}$$

Note that we only achieve equality in the constraint (10) if the corresponding D2D link is selected (active) and assigned one subband accordingly. The considered resource allocation problem can now be formulated as

$$\begin{aligned} \max_{\mathbf{p}, \boldsymbol{\rho}} \quad & \mathcal{R} = \sum_{k \in \mathcal{K}_c} \alpha r_k(\mathbf{p}, \boldsymbol{\rho}) + \sum_{k \in \mathcal{K}_d} (1 - \alpha) r_k(\mathbf{p}, \boldsymbol{\rho}) \\ \text{subject to} \quad & (4), (5), (6), (7), (8), (9), (10), (11), \end{aligned} \tag{12}$$

where α is a weight parameter that controls spectrum sharing of cellular and D2D links.

To solve this problem, we first investigate the optimal power allocation solution for a given subband assignment based on which we can develop subband assignment algorithms.

[1] Each subband can be a carrier and sub-channel in the multi-carrier wireless networks (e.g., LTE-based wireless networks).

[2] Extension to the case where each link can be allocated multiple subbands is discussed in Section V.C.

[3] In practice, it can be infeasible to support these minimum rate constraints. In this work, we assume, however, that these constraints can always be supported.

III. Optimal Power Allocation Algorithm

Note that we allow each cellular and active D2D link to use only one subband in the problem formulation (12). Therefore, if link $m \in \mathcal{K}$ is allocated subband n exclusively then the optimal power for this link is $P_m^{\max}$ and the corresponding contribution of this link to the objective value is

$$w_m^{[n]} \triangleq \begin{cases} \alpha \log_2\left(1+\frac{P_m^{\max} h_{mm}^{[n]}}{\sigma_m^{[n]}}\right) & \text{if } m \in \mathcal{K}_c \\ (1-\alpha)\log_2\left(1+\frac{P_m^{\max} h_{mm}^{[n]}}{\sigma_m^{[n]}}\right) & \text{if } m \in \mathcal{K}_d. \end{cases} \quad (13)$$

However, if cellular link k and D2D link l share subband n then the optimal power allocation must be determined from the following optimization problem[4]

$$\begin{aligned} \max_{p_{Ck}^{[n]},\ p_{Dl}^{[n]}} \quad & w_{kl}^{[n]} \triangleq \alpha r_{Ck}^{[n]} + (1-\alpha) r_{Dl}^{[n]} \\ \text{s.t.} \quad & r_{Ck}^{[n]} \geq R_k^{\min},\ r_{Dl}^{[n]} \geq R_l^{\min} \\ & p_{Ck}^{[n]} \in [0, P_k^{\max}],\ p_{Dl}^{[n]} \in [0, P_l^{\max}], \end{aligned} \quad (14)$$

where $r_{Ck}^{[n]} = \log_2\left(1+\frac{p_{Ck}^{[n]} h_{kk}^{[n]}}{\sigma_k^{[n]}+p_{Dl}^{[n]} h_{kl}^{[n]}}\right)$ and $r_{Dl}^{[n]} = \log_2\left(1+\frac{p_{Dl}^{[n]} h_{ll}^{[n]}}{\sigma_l^{[n]}+p_{Ck}^{[n]} h_{lk}^{[n]}}\right)$.

In fact, (14) presents the power allocation problem for weighted sum-rate maximization of two communication links. For this problem, it has been proved in [34] that if the problem is feasible then the optimal transmit powers $\mathbf{P} = (p_{Ck}, p_{Dl})$ have the form

$$\mathbf{P} \in \{(P_k^{\max}, p_{Dl}), (p_{Ck}, P_l^{\max})\}. \quad (15)$$

In [34], the authors consider maximizing the sum-rate of two interfering links without minimum rate constraints. For each possible optimal power allocation solution given in (15), the sum-rate objective function becomes a concave function of one variable and the optimal solution to maximize such a concave function belongs to the set of extreme points in the power set, i.e., $(0, P_l^{\max})$, $(P_k^{\max}, 0)$, or $(P_k^{\max}, P_l^{\max})$.

In contrast to [34], we deal with the maximization of the weighted sum rate of one D2D link and one cellular link with minimum rate constraints. To address this more complicated problem, we have to transform the weighted sum-rate objective function and the transformed function is neither concave nor convex as described in (36) of Appendix A. In addition, the feasible region of this constrained problem is more complicated than that of the problem in [34]. Hence, characterization of the optimal power allocation solution in this setting is more challenging.

Let us now define the following quantities:

$$P_{Dl}^{(1)} \triangleq \max\left\{\frac{(2^{R_l^{\min}}-1)(P_k^{\max} h_{lk}^{[n]} + \sigma_l^{[n]})}{h_{ll}^{[n]}},\ 0\right\} \quad (16)$$

$$P_{Dl}^{(2)} \triangleq \min\left\{\frac{1}{h_{kl}^{[n]}}\left(\frac{P_k^{\max} h_{kk}^{[n]}}{2^{R_k^{\min}}-1} - \sigma_k^{[n]}\right),\ P_l^{\max}\right\} \quad (17)$$

$$P_{Dl}^{(3)} \triangleq (-B_{Dl} + \sqrt{\triangle_{Dl}})/A_{Dl}, \quad (18)$$

[4]This power allocation problem aims at maximizing the contribution of the underlying subband assignment to the system weighted sum-rate.

where A_{Dl}, B_{Dl}, and $\triangle_{Dl}$ are specified in Appendix A. Then, the optimal power allocation solution of problem (14) is characterized in the following proposition whose proof is given in Appendix A.

Proposition 1. *If the optimal power allocation solution of problem (14) is in the form $(P_k^{\max}, p_{Dl})$ then it belongs the following set*

$$\mathcal{S}_1 \triangleq \begin{cases} \{(P_k^{\max}, P_{Dl}^{(1)}), (P_k^{\max}, P_{Dl}^{(2)}), (P_k^{\max}, P_{Dl}^{(3)})\}, \\ \qquad \textit{if } P_{Dl}^{(3)} \in [0, P_l^{\max}] \\ \{(P_k^{\max}, P_{Dl}^{(1)}), (P_k^{\max}, P_{Dl}^{(2)})\},\ \textit{otherwise}. \end{cases} \quad (19)$$

Similarly, let us define

$$P_{Ck}^{(1)} \triangleq \max\left\{\frac{(2^{R_k^{\min}}-1)(P_l^{\max} h_{kl}^{[n]} + \sigma_k^{[n]})}{h_{kk}^{[n]}},\ 0\right\} \quad (20)$$

$$P_{Ck}^{(2)} \triangleq \min\left\{\frac{1}{h_{lk}^{[n]}}\left(\frac{P_l^{\max} h_{ll}^{[n]}}{2^{R_l^{\min}}-1} - \sigma_l^{[n]}\right),\ P_k^{\max}\right\} \quad (21)$$

$$P_{Ck}^{(3)} \triangleq (-B_{Ck} + \sqrt{\triangle_{Ck}})/A_{Ck}, \quad (22)$$

where A_{Ck}, B_{Ck}, and $\triangle_{Ck}$ are calculated as

$$A_{Ck} = \frac{1}{\beta} h_{kk} h_{lk}^2,\ B_{Ck} = \frac{1-\beta}{2\beta} P_l^{\max} h_{ll} h_{lk} h_{kk} + \frac{1}{\beta}\sigma_l h_{lk} h_{kk},$$

$$C_{Ck} = \frac{1}{\beta}\sigma_l h_{kk}(\sigma_l + P_l^{\max} h_{ll}) - P_l^{\max} h_{ll} h_{lk}(\sigma_l + P_l^{\max} h_{kl}),$$

$$\triangle_{Ck} = B_{Ck}^2 - A_{Ck} C_{Ck},\ \beta = \frac{1-\alpha}{\alpha}.$$

Then, we have following results.

Proposition 2. *If the optimal power allocation solution of problem (14) is in the form $(p_{Ck}, P_l^{\max})$, then it belongs to the following set*

$$\mathcal{S}_2 \triangleq \begin{cases} \{(P_{Ck}^{(1)}, P_l^{\max}), (P_{Ck}^{(2)}, P_l^{\max}), (P_{Ck}^{(3)}, P_l^{\max})\}, \\ \qquad \textit{if } P_{Ck}^{(3)} \in [0, P_k^{\max}] \\ \{(P_{Ck}^{(1)}, P_l^{\max}), (P_{Ck}^{(2)}, P_l^{\max})\},\ \textit{otherwise}. \end{cases} \quad (23)$$

Proof. The proof is omitted due to the space constraint. ■

Combining the results in Propositions 1 and 2, we can characterize the optimal solution structure of problem (14) in the following theorem.

Theorem 1. *If the problem (14) is feasible then its optimal power allocation solution belongs to the set $\mathcal{S}^* \triangleq \mathcal{S}_1 \bigcup \mathcal{S}_2$.*

Since $\mathcal{S}^*$ contains at most 6 possible power allocation solutions, we can determine the optimal solution by examining all potential solutions in $\mathcal{S}^*$ easily. Therefore, the optimal contribution to the system weighted sum-rate for each subband n due to exclusive and co-sharing solutions in (13) and (14), denoted as $w_m^{[n]}$ and $w_{kl}^{[n]}$, respectively, can be determined accordingly. If problem (13) or (14) is not feasible, we will set $w_m^{[n]} = -Q$ or $w_{kl}^{[n]} = -Q$ where Q is a sufficiently large number so that link m or the pair of D2D link k and cellular link l is not assigned subband n.

IV. Subband Assignment Algorithms

A. Graph-based Resource Allocation Formulation

Since optimal power allocation for a given subband assignment can be determined as in the previous section, problem (12) can be transformed to the subband assignment problem. We propose to solve the subband assignment problem by using the graph-based approach where each link or subband can be modeled as a vertex, and one subband assignment corresponds to one hyper-edge in the graph. This design is presented in more details in the following.

1) Graph-based Model: We now describe how all design requirements and constraints of the resource allocation problem can be modeled. The constraint (9) means that each cellular link must be allocated one subband. To fulfill this requirement, we introduce $\mathcal{K}_{cv} = \{0_{c_1}, 0_{c_2}, \cdots, 0_{c_{N_d}}\}$ as the set of $N_d = (N - K_c)$ virtual cellular links. Then, the number of cellular links (actual and virtual cellular links) is equal to the number of subbands. The introduction of virtual cellular links, therefore, enables us to model the subband assignment problem as the one-one matching between cellular links and subbands, which guarantees that each cellular link is assigned one subband. Furthermore, we introduce a single virtual D2D link 0_d and also define $\mathcal{K}_{dv} = \{0_d\}$. For convenience, we also define the sets $\mathcal{K}_C \triangleq \mathcal{K}_c \cup \mathcal{K}_{cv}$ and $\mathcal{K}_D \triangleq \mathcal{K}_d \cup \mathcal{K}_{dv}$.

Now, we define the sets of vertexes and hyper-edges of the graph as follows:

$$V^0 = \{k, l, n|\ k \in \mathcal{K}_C, l \in \mathcal{K}_D, n \in \mathcal{N}\} \quad (24)$$

$$E^0 = \{e = (k, l, n)|\ k \in \mathcal{K}_C, l \in \mathcal{K}_D, n \in \mathcal{N}\}, \quad (25)$$

where V^0 is the set of vertexes whose elements are the cellular links, D2D links, and subbands; and E^0 is the set of hyper-edges where each hyper-edge $e = (k, l, n) \in E^0$ corresponds to the assignment of subband n to cellular link k and D2D link l. For simplicity, we call *edges* instead of *hyper-edges* in the sequel. Determination of the subband assignment solution is then equivalent to determining a subset of edges in this graph, which satisfies all constraints of the resource allocation problem and maximizes the weighted sum-rate. It is clear that if the final solution chooses an edge corresponding to cellular link k, virtual D2D link 0_d, and subband n then this cellular link k uses subband n exclusively. It can be observed that a single virtual D2D link 0_d is sufficient for our design purpose if this virtual D2D link 0_d can be matched with multiple cellular links on the corresponding different subbands in the final solution. Similarly, if a particular D2D link l is matched with one virtual cellular link on subband n then this D2D link l uses subband n exclusively.

Fig. 1 illustrates this graph representation where the edges represent the corresponding subband assignments. Recall that edge $e = (k, l, n)$ corresponds to the assignment of subband n to cellular link k and D2D link l whose contribution w_e to the weighted sum-rate (the design objective) can be determined through the optimal power allocation in (13) and (14) for exclusive and sharing subband assignments, respectively.[5] By

[5]Specifically, we have $w_e = w_m^{[n]}$ for exclusive subband assignment in (13) and $w_e = w_{kl}^{[n]}$ for sharing subband assignment in (14).

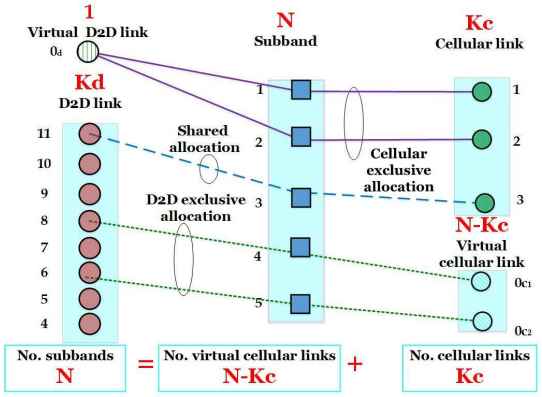

Fig. 1. Hyper-edge and vertex presentation of the subband assignment problem

using the results in the previous section, we can determine the weights w_e for all possible subband assignments.

2) Subband Assignment Problem: Let $V(E)$ be the set of vertexes associated with the set of edges E. We denote $V_c(E)$, $V_d(E)$, and $V_n(E)$ are the sets of actual cellular links, D2D links, and subbands in the set of vertexes $V(E)$, respectively. To describe the subband assignment decision, we introduce a binary variable x_e where x_e=1 means edge e is activated (i.e., the corresponding subband allocation is made) and x_e=0, otherwise. Moreover, let $\mathbf{x}$ denote the vector whose elements are subband assignment variables x_e associated with all possible edges. In addition, the degree of vertex v in the set of edges E associated with $\mathbf{x}$ can be defined as

$$D(v, E) \triangleq \sum_{e \in E(v)} x_e, \quad (26)$$

where $E(v)$ is the set of edges containing vertex v.

Suppose that we have determined the subband assignments for all subbands and let E denote the set of only active edges with x_e = 1. Then, $D(v, E), v \in V_d(E)$ and $D(v, E), v \in V_c(E)$ describe the number of subbands allocated to D2D link v and cellular link v, respectively. Similarly, $D(v, E), v \in \mathcal{N}$ is the number of link pairs (D2D and cellular links) using subband $v \in \mathcal{N}$. Therefore, the subband assignment problem can be reformulated into the following integer programming problem $\mathbf{IP}(V, E)$

$$\begin{aligned} \max_{x_e} \quad & \mathcal{R} = \sum_{e \in E} w_e x_e \\ \text{s.t.} \quad & C1:\ D(v, E) = 1\ \forall v \in V \cap K_C \\ & C2:\ D(v, E) \le 1\ \forall v \in V_d(E) \cup V_n(E) \\ & C3:\ x_e \in \{0, 1\}\ \forall e \in E. \end{aligned} \quad (27)$$

In problem (27), constraints C1 implies that each cellular link v (both actual and virtual links) must be allocated exactly one subband, which guarantees its required minimum rate. In addition, constraints C2 ensure that each D2D link v is assigned at most one subband, and each subband is shared by at most one pair of cellular-D2D links. Constraints C2 allow us to capture two possible outcomes for each D2D link,

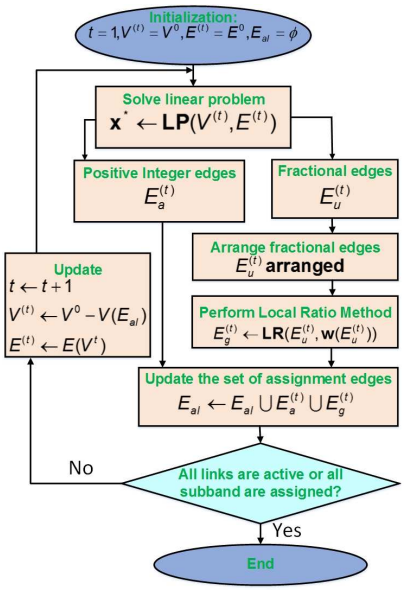

Fig. 2. The flowchart of Iterative Rounding Algorithm

i.e., it is allocated one subband if it is selected (active) or it is not allocated any subband if it is not selected (inactive). This explains the need to use inequality instead of equality constraints in C2. Note also that the constraint C2 is not applied to the virtual D2D link 0_d since its degree can be greater than 1, i.e., there are multiple cellular links using their allocated subbands exclusively.

For problem $\mathbf{IP}(V, E)$, if we relax the integer allocation constraint $x_e \in \{0, 1\}\ \forall e \in E$ to $x_e \in [0, 1]\ \forall e \in E$ then we obtain the corresponding linear relaxation problem, which is refereed to as $\mathbf{LP}(V, E)$ in the sequel. Note that $\mathbf{IP}(V^0, E^0)$ corresponds to the original subband allocation problem, which is challenging to address since there may not exist a polynomial-time algorithm to solve it. To overcome this challenge, we propose two algorithms to solve problem $\mathbf{IP}(V^0, E^0)$ in the following, namely Iterative Rounding algorithm, and optimal BnB algorithm.

B. Iterative Rounding Algorithm

1) Outline of Design Principals: It can be observed that the linear relaxation problem $\mathbf{LP}(V^0, E^0)$ can be solved easily by standard optimization solutions, i.e., simplex or interior point method [35]. However, solving problem $\mathbf{LP}(V^0, E^0)$ often results in fractional values for some edges e $(0 < x_e < 1)$. To address this issue, we propose an Iterative Rounding Algorithm in which we solve a linear relaxation problem and perform suitable rounding for fractional variables in each iteration. This is repeated until all links are active or all subband are allocated.

Specifically, the Iterative Rounding Algorithm performs the following operations in three phases of each iteration t. In phase 1, it solves the linear relaxation problem for inactive links and available subbands corresponding to the graph with the set of vertexes $V^{(t)}$ and the set of edges $E^{(t)}$, which results in two sets of variables equal to fractional values $(0 < x_e < 1)$ and one $(x_e = 1)$, namely $E_a^{(t)}$ and $E_u^{(t)}$, respectively. We then arrange the edges in the set $E_u^{(t)}$ with fractional subband assignment variables in phase 2 based on which we employ the Local Ratio Method in phase 3 to determine the set of additional subband assignments $E_g^{(t)}$. Phases 2 and 3 have been indeed appropriately designed to minimize the performance loss due to rounding of the fractional subband assignment variables. The edges in $E_a^{(t)} \cup E_g^{(t)}$ will be used to perform the corresponding subband assignments for cellular and/or D2D links in each iteration. Finally, we update the set of available subbands and inactive links and go back to phase 1 of the next iteration until convergence. The main operations of the algorithm are illustrated in Fig. 2.

2) Resource Allocation Algorithm: Detailed operations of the Iterative Rounding Algorithm are presented in Algorithm 1. In each iteration t, we have to solve a subband assignment problem formulated in (27) whose underlying graph is formed by the sets of vertexes and edges $(V^{(t)}, E^{(t)})$, i.e., $V = V^{(t)}, E = E^{(t)}$, which is a sub-graph of original graph with the corresponding sets (V^0, E^0). We initialize the algorithm with $V^{(t)} = V^0, E^{(t)} = E^0$ in the first iteration $t = 1$. Moreover, we use E_{al} to denote the set of edges corresponding to all subband assignments accumulated over iterations. The operations of three phases conducted in each iteration t are described in the following.

Algorithm 1 Iterative Subband Assignment Algorithm

1: Initialization $t = 1$, $E_{al} = \emptyset$, $V^{(t)} = V^0$, $E^{(t)} = E^0$
2: **while** $V_n(E_{al}) \neq \mathcal{N}$ and $V_c(E_{al}) \cup V_d(E_{al}) \neq \mathcal{K}_c \cup \mathcal{K}_d$ **do**
3: Phase 1:
4: Solve $\mathbf{x}^* = \text{argmax}\, \mathbf{LP}(V^{(t)}, E^{(t)})$.
$E_a^{(t)} = \{e \in E^{(t)} | x_e^* = 1\}$, $E_u^{(t)} = \{e \in E^{(t)} | 0 < x_e^* < 1\}$.
5: Phase 2:
Set $E_{ua}^{(t)} \leftarrow \emptyset$, $E_{uu}^{(t)} \leftarrow E_u^{(t)}$.
6: **for** i = 1 **to** $|E_u^{(t)}|$ **do**
7: $e^* = \underset{e \in E_{uu}^{(t)}}{\text{argmin}}\, c(E_{uu}^{(t)}, e)$.
$E_{ua}^{(t)} \leftarrow E_{ua}^{(t)} \cup e^*$.
$E_{uu}^{(t)} \leftarrow E_{uu}^{(t)} - e^*$.
8: **end for**
$E_u^{(t)} \leftarrow E_{ua}^{(t)}$
9: Phase 3:
10: $E_g^{(t)} \leftarrow \mathbf{LR}(E_u^{(t)}, \mathbf{w}(E_u^{(t)}))$.
11: $E_{\text{al}} = E_{\text{al}} \cup E_a^{(t)} \cup E_g^{(t)}$.
$t \leftarrow t + 1$.
Update $V^{(t)} \leftarrow V^0 - V(E_{al})$ and $E^{(t)} = E(V^{(t)})$.
12: **end while**
13: Output E_{al} and perform subband assignments according to the edges in set E_{al}.

a) Linear Relaxation Phase: In this phase, we solve the linear programming relaxation problem $\mathbf{LP}(V^{(t)}, E^{(t)})$ (line 4 in Algorithm 1), and obtain two sets of subband assignment variables whose values are fractional (smaller than 1) and equal to one, respectively. Specifically, let $\mathbf{x}^*$ denote the optimal solution of problem $\mathbf{LP}(V^{(t)}, E^{(t)})$ then we define these two sets as

$$E_a^{(t)} = \{e \in E^{(t)} | x_e^* = 1\} \quad (28)$$

$$E_u^{(t)} = \{e \in E^{(t)} | 0 < x_e^* < 1\}, \quad (29)$$

Algorithm 2 $\mathbf{LR}(E, \mathbf{w}(E))$

1: $E_{\mathsf{temp}} \leftarrow \emptyset$, $j = 1$.
2: **repeat**
3: Choose from E the smallest index edge e^*.
4: $e_j \leftarrow e^*$
5: Update $E_{\mathsf{temp}} \leftarrow E_{\mathsf{temp}} \cup e_j$ and $j \leftarrow j + 1$
6: For each edge $e' \in E \cap E(V(e))$,
1. Update the weight value $w_{e'} \leftarrow w_{e'} - w_{e^*}$.
2. If $w_{e'} \leq 0$, $E \leftarrow E - e'$
7: **until** $E = \emptyset$
8: $E_s^{(|E_{\mathsf{temp}}|+1)} = \emptyset$
9: **for** $j = |E_{\mathsf{temp}}|$ **to** 1 **do**
10: Choose edge $e_j \in E_{\mathsf{temp}}$ to do the following
If $V(e_j) \cap V(E_s^{(j+1)}) = \emptyset$, $E_s^{(j)} \leftarrow E_s^{(j+1)} \cup e_j$, else $E_s^{(j)} \leftarrow E_s^{(j+1)}$.
11: **end for**
12: Return $E_s^{(1)}$.

which are associated with $\mathbf{LP}(V^{(t)}, E^{(t)})$. We define $V_u^{(t)} = V(E_u^{(t)})$ and $V_a^{(t)} = V(E_a^{(t)})$ as the sets of vertexes associated with $E_a^{(t)}$ and $E_u^{(t)}$, respectively. We refer to edges in the set $E_u^{(t)}$ as fractional edges in the sequel. To proceed further, let $E(V)$ represent the set of edges each of which has at least one of its vertexes in the set V. Based on $\mathbf{x}^*$, we obtain the assignment vectors $\mathbf{x}_a^*$ and $\mathbf{x}_u^*$ corresponding to edges in the sets $E(V_a^{(t)})$ and $E(V_u^{(t)})$, respectively. Now, $E_u^{(t)}$ and $\mathbf{x}_u^*$ are used in the following two phases to determine additional subband assignments.

b) Fractional Edge Arrangement Phase: The objective of this phase is to arrange the fractional edges, which helps select additional edges for further subband assignments (lines 6-8 Algorithm 1). Toward this end, we define a coupling parameter $c(e, E)$ for each fractional edge e as

$$c(e, E) \triangleq \sum_{e' \in E \cap E(V(e))} x_{e'}^*, \tag{30}$$

where $V(e)$ is the set of vertexes of edge e. In fact, $c(e, E)$ represents the sum of fractional values of edges in set E that have at least one common vertex with edge e. In this phase, we arrange the edges in $E_u^{(t)}$ in the ascending order of their coupling parameters. Specifically, the edge arrangement procedure is executed as follows. Initially, $c(e, E_u^{(t)})$ is calculated for all edges $e \in E_u^{(t)}$. Then, the edge having smallest coupling parameter is selected and removed from $E_u^{(t)}$. These procedure is repeated until all the edges in $E_u^{(t)}$ is arranged. Moreover, we assume that edges are indexed in the order they are added to set $E_{ua}^{(t,i)}$ in line 7 of Algorithm 1. The set of arranged edge $E_u^{(t)}$ is used for the next phase of the algorithm.

c) Local Ratio Rounding Phase: In the third phase, we employ the *Local Ratio Method* [32] to assign the remaining bandwidth resources to fractional edges, which is described in Algorithm 2, $\mathbf{LR}(E, \mathbf{w}(E))$. The way these assignments are performed can be explained as follows. The rearranged edges obtained at the end of phase two of Algorithm 1 are considered sequentially to perform further subband assignments in the order of increasing indexes of $E_u^{(t)}$. The idea is that if we sequentially round up edges starting from those with smallest coupling parameters and perform corresponding subband assignments then this rounding operation would minimize the impacts to other unallocated edges and therefore the performance loss.

At the end of each iteration t, we obtain the set $E_g^{(t)}$, which contains edges corresponding further subband assignments. Finally, $E_a^{(t)}$ and $E_g^{(t)}$ are added to the "assignment" set E_{al} at the end of each iteration (line 11 in Algorithm 1). In Algorithm 2 $\mathbf{LR}(E, \mathbf{w}(E))$ where $\mathbf{w}(E)$ is the original weighted vector corresponding to the edges in E, in which w_e is the weighted value of edge e obtained from the optimal power allocation described in Section III. As we consider a particular edge e, we decrease the weight of each coupled edge e' of e by w_e (line 6). Here, edges e' and e are defined to be coupled if they share at least one vertex and we assume that e is coupled with itself. After these weight updates, any edges with non-positive weights will be excluded from being added to set $E_g^{(t)}$. In the end, we exclude some further edges so that each edge in the returned set $E_s^{(1)}$ is not coupled with any other edges in this set (lines 9-11 of Algorithm 2).

3) Properties of Iterative Rounding Algorithm: Firstly, we state an important property related to the linear relaxation phase.

Proposition 3. *$\mathbf{x}_u^*$ is also an optimal solution of problem $\mathbf{LP}(V_u^{(t)}, E(V_u^{(t)}))$.*

Recall that $V_u^{(t)}$ is the set of vertexes corresponding to the fractional edges, and $E(V_u^{(t)})$ is the set of edges each of which has at least one of its vertexes in $V_u^{(t)}$.

Proof. The proof is given in Appendix B. ■

The results in Proposition 3 are very useful because it implies that one can split the linear programming problem $\mathbf{LP}(V^{(t)}, E^{(t)})$ into two linear programming problems $\mathbf{LP}(V_u^{(t)}, E(V_u^{(t)}))$ and $\mathbf{LP}(V_a^{(t)}, E(V_a^{(t)}))$ of smaller size. In addition, problem $\mathbf{LP}(V_a^{(t)}, E(V_a^{(t)}))$ has the integer optimal solution and problem $\mathbf{LP}(V_u^{(t)}, E(V_u^{(t)}))$ has the fractional optimal solution. Consequently, we can perform subband assignments corresponding to the edges in $E_a^{(t)}$ which provides one part of the final subband assignment solution. Moreover, we only need to solve problem $\mathbf{LP}(V_u^{(t)}, E(V_u^{(t)}))$ to determine further subband assignments.

In addition, we need to investigate the solution obtained from each iteration of the algorithm. To facilitate the description, let we denote $z(E) = \sum_{e \in E} w_e$ as total weight of all edges in E, and $l^*(V, E)$ be the optimal objective value of problem $\mathbf{LP}(V, E)$. At each iteration t, we perform the rounding operations to obtain set $E_g^{(t)}$ based on the solution of problem $\mathbf{LP}(V_u^{(t)}, E(V_u^{(t)}))$.

Proposition 4. *The total weight of selected edges in set $E_g^{(t)}$ (line 10 of Algorithm 1) is at least half of the optimal objective of the linear relaxation problem, i.e., $z(E_g^{(t)}) \geq \frac{1}{2} l^*(V_u^{(t)}, E(V_u^{(t)}))$.*

Proof. The proof is given in Appendix C ■

The above proposition characterizes the achieved objective in each iteration t. We now state the main results that char-

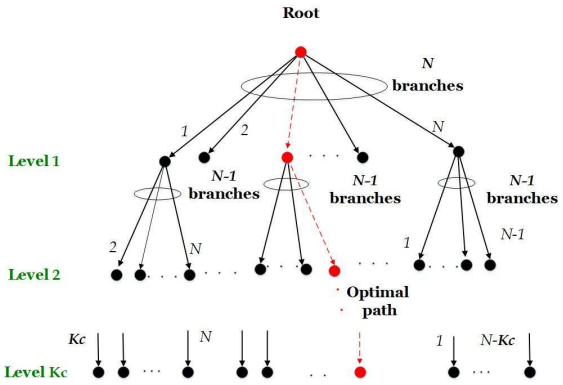

Fig. 3. Tree structure of BnB algorithm

acterize the performance guarantee of Algorithm 1. The proof is given in Appendix D.

Proposition 5. *A feasible solution of the original subband allocation problem* $\mathbf{IP}(V^0, E^0)$*, offered by Algorithm 1, achieves at least half of the optimal objective value of the linear relaxation problem* $\mathbf{LP}(V^0, E^0)$.

This proposition implies that we can always guarantee that Algorithm 1 achieves at least 1/2 optimal objective value. This is true even if the solution of problem $\mathbf{LP}(V^0, E^0)$ corresponds all fractional edges.

C. Branch and Bound Algorithm

We now describe an optimal Branch and Bound (BnB) algorithm with novel branching and bounding procedures to limit the search complexity.

1) Branching: We propose to branch the solution space over a tree comprising K_c levels where each level corresponds to one cellular link as demonstrated in Fig. 3. Each node n at level k in the tree represents one potential assignment of subband n to cellular link k. Since each subband can be allocated to at most one cellular link, we remove the underlying subbands from the next-level allocations associated with their child nodes. Therefore, the number of branches originated from each node decreases over the tree levels. The objective of the BnB algorithm is to determine an optimal path through the tree which corresponds to optimal subband assignments.

In general, at each level k, we can branch up to $K_d N$ nodes where each node corresponds to the sharing of cellular link k and D2D link l on subband n. Note that in our proposed tree structure, each node at level k presents the subband assignment for cellular link k, which is independent of the subband assignment for D2D links. Therefore, our branching procedure effectively reduces the search complexity.

2) Bounding: To reduce the search complexity, we remove sub-trees originating from some particular nodes if subband allocations corresponding to these sub-trees cannot belong to the potential optimal path. To facilitate these sub-tree removals, we maintain a global lower-bound Z_{int} which corresponds to the current best feasible solution. Moreover in each visited node, we calculate the local upper-bound B_{ul} which presents an upper-bound of the objective value for the optimal solution containing the visited node. If we have $Z_{\mathsf{int}} > B_{ul}$ at any node then the sub-tree formed by the child nodes of the underlying node will be removed from future considerations.

For a particular node n at level k_0, there is a unique path from this node to the root, which provides the sets of active cellular links and their allocated subbands, denoted as $V_{ca} \triangleq \{1, \cdots, k_0\}$ and $V_{na} \triangleq \{n_1, \cdots, n_{k_0}\}$, respectively. The local upper-bound B_{ul} for node n_k at level k can be calculated by solving problem $\mathbf{LP}(V^0, E^0)$ with the following constraints

$$D(k, E(n_k)) = 1 \ \forall k \in V_{ca}, \tag{31}$$

which force subband n_k to be allocated to cellular link k for all $k \in V_{ca}$.

We develop an algorithm to find a feasible solution at level K_c, which can be used to update Z_{int} as follows. Note that at level K_c all cellular links are active. Therefore, problem $\mathbf{IP}(V^0, E^0)$ degenerates into the resource allocation problem of D2D links. We assume that subband $n \in \mathcal{N}$ is allocated for cellular link $k_n \in \mathcal{K}_C$ where k_n can be a virtual cellular link. Hence, if subband n is allocated to D2D link l, the weighted sum rate gain can be calculated as

$$q_l^n = \begin{cases} w_l^{[n]} & \text{if } k_n \in \mathcal{K}_{cv} \\ w_{k_n l}^{[n]} - w_{k_n}^{[n]} & \text{if } k_n \in \mathcal{K}_c, \end{cases} \tag{32}$$

where $w_l^{[n]}$, $w_{k_n}^{[n]}$ and $w_{k_n l}^{[n]}$ are the weighted value of D2D link l if it uses subband n exclusively; weighted value of cellular link k_n if it uses subband n exclusively; and weighted value for cellular link k_n and D2D link l on subband n, respectively. Hence, problem $\mathbf{IP}(V^0, E^0)$ can be transformed to the following problem

$$\begin{aligned} \max_{\mathbf{y}} \quad & \sum_{l \in \mathcal{K}_d} \sum_{n \in \mathcal{N}} q_l^n y_{ln} \\ \text{s.t.} \quad & C1: \ \sum_{n \in \mathcal{K}_d} y_{ln} \leq 1 \ \forall l \in \mathcal{K}_d \\ & C2: \ \sum_{l \in \mathcal{N}} y_{ln} \leq 1 \ \forall n \in \mathcal{N} \\ & C3: \ y_{ln} \in \{0, 1\} \ \forall n \in \mathcal{N} \ \forall l \in \mathcal{K}_d, \end{aligned} \tag{33}$$

where $\mathbf{y}$ represents the subband assignment vector of all D2D links. This problem belongs to the class of job assignment problem, which can be solved efficiently by the Hungarian method [36]. Denote $\mathbf{y}^0$ and $\mathcal{R}^0$ as the assignment vector of D2D links and objective value obtained by the Hungarian method. Hence, the objective value of problem $\mathbf{IP}(V^0, E^0)$ can be expressed as $Z_{\mathsf{current}} = \mathcal{R}^0 + \sum_{n \in V_{na}} (\sum_{l \in \mathcal{K}_d} y_{ln}^0) w_{k_n}^{[n]}$. Therefore, if $Z_{\mathsf{current}} > Z_{\mathsf{int}}$, we can update the global lower-bound as $Z_{\mathsf{int}} \leftarrow Z_{\mathsf{current}}$. Finally, we search over the proposed tree until all nodes have been solved or excluded to determine the optimal path (i.e., optimal subband assignments).

V. Complexity Analysis and Extensions

A. Complexity Analysis

The computational complexity is analyzed by counting the number of operations required in the power allocation and

subband assignment phases, but the complexity of the power allocation phase is indeed negligible. In the Iterative Rounding algorithm, the number of iterations is O(1). In the first iteration, the computational complexity is dominated by the complexity required to solve the linear program. The primal dual interior-point method employed to solve this problem has complexity of $O\left((K_C K_D N)^{3.5}\right)$, where $K_C K_D N$ is the number of variables [35, p. 324]. The complexity of fractional edge arrangement phase and local ratio rounding phase is negligible; Therefore, the overall computational complexity of the Iterative Rounding algorithm is $O\left((K_C K_D N)^{3.5}\right)$.

The computational complexity of the BnB algorithm depends on the operations conducted by each node and the number of visited nodes. The complexity of the Hungarian method, which is employed to solve the job assignment and linear programming problems is $O(M^{3.5})$ where M is the number of variables. The worst-case complexity of the BnB algorithm can be calculated based on the maximum number of visited node, which is $\frac{N!}{(N-K_c)!}$. In addition, the complexity of running the Hungarian method are $O\left((\max\{K_c, K_d, N\})^3\right)$ [36], which is much smaller than $O(K_C K_D N)^{3.5}$. Hence, the complexity of the BnB algorithm is $O(\frac{N!(K_C K_D N)^{3.5}}{(N-K_c)!})$. Note that the complexity of the exhaustive search algorithm is $O(\frac{N!N!}{(N-K_c)!(N-K_d)!})$ if $N > K_d$ and $O(\frac{N!K_d!}{(N-K_c)!(K_d-N)!})$ if $N < K_d$. Therefore, for sufficiently large values of K_d and N (e.g., $N, K_d > 10$), the BnB algorithm is significantly more efficient than the exhaustive search algorithm.

B. Further Extensions

We now address the more general case where each cellular or D2D link can be allocated multiple subbands (scenario II). We adopt the two-step approach to perform resource allocation for this general case. In the first step, we determine the number of subbands that must be allocated to each link m, denoted as N_m, by using certain bandwidth allocation approach. Then, we can employ the proposed resource allocation framework presented previously to address the design in the second step as follows. We map each link m to N_m new equivalent links, each of which has the maximum transmit power $P_m^{\max}/N_m$, and the minimum required data rate $R_m^{\min}/N_m$. We then apply the proposed resource allocation algorithms for the equivalent system with more links. Finally, the assigned subbands and the corresponding powers for each link m can be determined from the resource allocation solutions for its N_m links.

VI. Numerical Results

A. Simulation Setting

We consider the simulation setting illustrated in Fig. 4 where there is a single BS with the coverage area of 500m serving $K_c = 20$ randomly distributed cellular users. Moreover, there are $N = 25$ subbands, which are shared by $K_c = 20$ cellular links and $K_d = 30$ D2D links unless stated otherwise. The D2D transmitters are randomly distributed in the cell area, and each D2D receiver is randomly located in the area close to its D2D transmitter within the maximum distance of $d_{\max}$. The channel power gain is modeled as $h_{kl}^{[n]} = d_{kl}^{-\gamma}\delta$ where

TABLE II
Simulation Parameters

Description	Parameter	Value
Number of cellular links	K_c	10, 20
Number of D2D links	K_d	10, 25, 30, 50
Number of subbands	N	25
Path loss exponent	γ	3
Maximum distance between Tx and Rx of D2D links	$d_{\max}$	80m
Maximum transmitted power	$P_c^{\max}$, $P_d^{\max}$	0.5W
Minimum required rate	$R_c^{\min}$, $R_d^{\min}$	3b/s/Hz
Weight parameter	α	0.5
Noise power	σ_k	10^{-13}

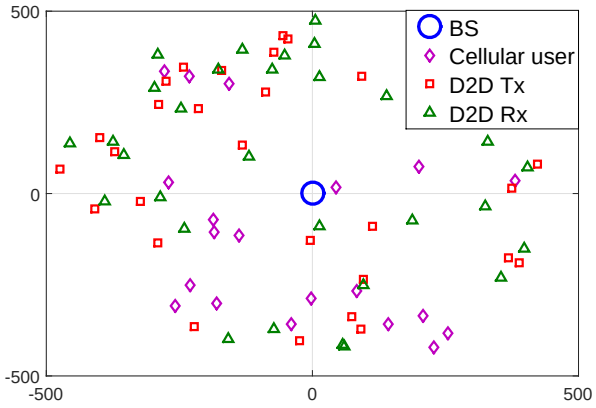

Fig. 4. Simulation setting

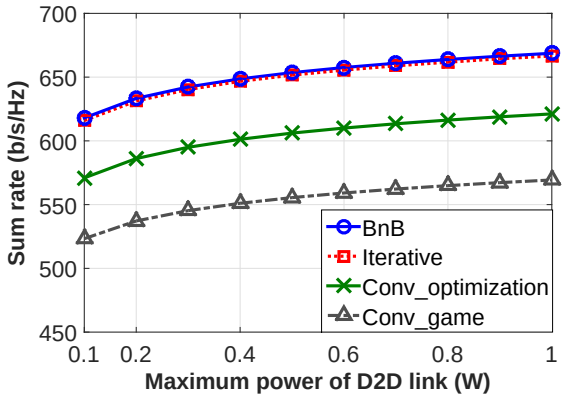

Fig. 5. System sum rate versus $P_d^{\max}$ as $K_c = 10$

d_{kl} is the distance between the receiver of link k and the transmitter of link l; δ represents the Rayleigh fading, which follows exponential distribution with the mean value of 1. The values of parameters for our simulation are summarized in Table II unless stated otherwise.

B. Numerical Results for Scenario I

We compare the performance of our proposed algorithms with conventional algorithms developed for scenario I in [13] and [14]. The first conventional algorithm, refereed to as the optimization-based conventional algorithm, performs the resource allocation in three phases. In the first phase, the matching between cellular and D2D links is executed based on the relative distance between cellular transmitter and D2D

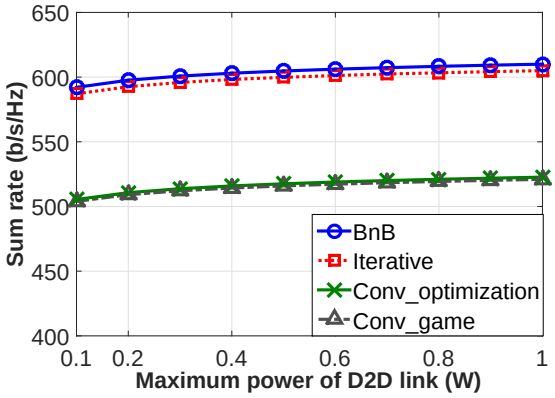

Fig. 6. System sum rate versus $P_d^{\max}$ as $K_c = 20$

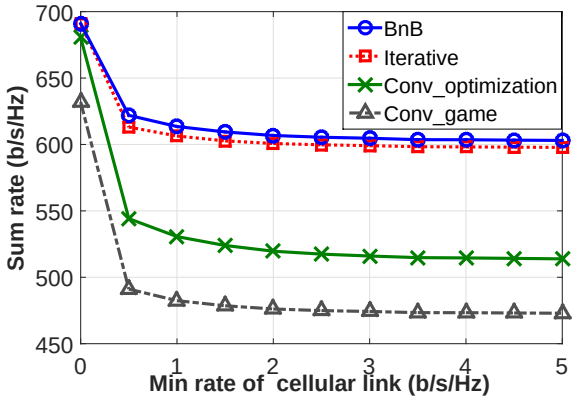

Fig. 7. Sum rate versus minimum rate of each cellular link

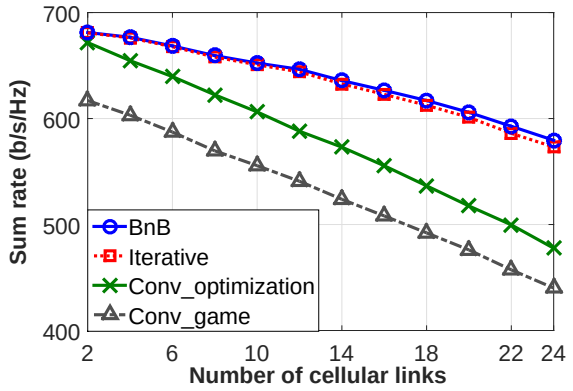

Fig. 8. System sum rate versus K_c as $K_d = 30$

receiver. Then, in the second phase, the power allocation for a pair of cellular and D2D links is performed to achieve the optimal weighted sum-rate of both links. Finally, the matching between the subbands and different pairs of links is determined by using the Hungarian method. In contrast to the algorithm in [13], the work [14] adopted a game-based approach where the resource allocation for cellular links is determined first. Then, the optimal power allocation for each pair of cellular and D2D links is calculated. Finally, the matching between D2D links and the resources of cellular links is decided by using the stable matching and cheating technique [37].

In the following, all numerical results are obtained by averaging over 1000 random realizations of D2D, cellular locations, and channel gains. The results corresponding to the BnB, Iterative Rounding, optimization-based conventional, and game-based conventional algorithms are indicated by "BnB", "Iterative", "Conv_optimization", and "Conv_game" in all figures, respectively.

Figs. 5 and 6 illustrate the system sum-rate versus the maximum power of each D2D link as $K_c = 10$ and $K_c = 20$, respectively. It shows that the system sum-rate increases moderately as the D2D maximum power becomes larger. This is because short-range D2D links do not require very large transmit power to achieve high date rates compared to the cellular links. Moreover, the D2D power budget is mainly used to combat the interference from cellular links, which interprets the moderate gain in system sum-rate. It is remarkable that the Iterative Rounding algorithm performs extremely well and its achieved sum-rate is almost the same as that due to the optimal BnB algorithm. The Iterative Rounding algorithm indeed performs quite better than the worst-case performance bound stated in Proposition 5. This is because the worst-case bound assumes that the linear relaxation phase results in all fractional edges and the worst performance loss in the rounding phase.

Moreover, the Optimization-based conventional algorithm performs better than the Game-based conventional algorithm as $K_c = 10$. This is due to the fact that the Optimization-based conventional algorithm jointly optimizes the subband assignments for both cellular and D2D links while the Game-based conventional algorithm performs subband assignments for cellular links and D2D links in two separate steps which results in the significant performance loss.

In Fig. 7, we demonstrate the system sum-rate versus the minimum required rate of cellular links $R_c^{\min}$. It can be seen that the system sum-rate reaches the maximum value as $R_c^{\min} = 0$. This is because when as $R_c^{\min} = 0$, D2D links have more advantages than cellular links in accessing good subbands thanks to the short-range of D2D links. Hence, the rate of D2D links become higher for the smaller minimum required rate of each cellular link. It can also be observed that the system sum-rate decreases significantly as $R_c^{\min}$ increases from zero before getting saturated at fixed value.

Fig. 8 shows the variations of the system sum-rate with the number of cellular links K_c as we fix $K_d = 30$. This figure demonstrates that the system sum-rate decreases with the number of cellular links. In fact, as K_c increases, the number of active D2D links is reduced, which results in the decrease in the system sum-rate. In addition, Fig. 9 demonstrates the system sum-rate versus K_c as we fix $K_d = 10$. As shown in this figure, the system sum-rate first increases then decreases with K_c, which can be explained as follows. As K_c is small, increasing K_c does not significantly impact the data rates of D2D links since all D2D links can still exploit the subbands exclusively. Moreover, larger number of cellular links can result in better spectrum utilization, which improves the system sum-rate. However, when K_c is sufficiently large, increasing K_c leads to the scenario where active D2D links must share subbands with cellular links and the number of

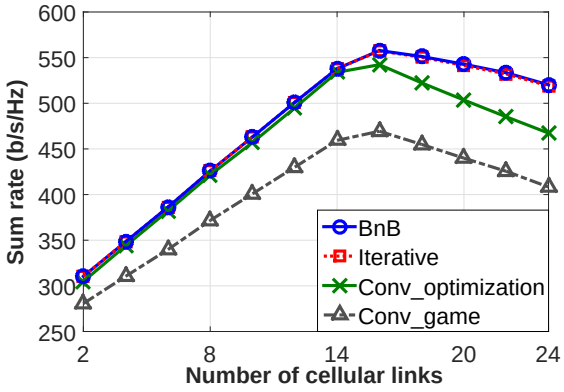

Fig. 9. System sum rate versus K_c as $K_d = 10$

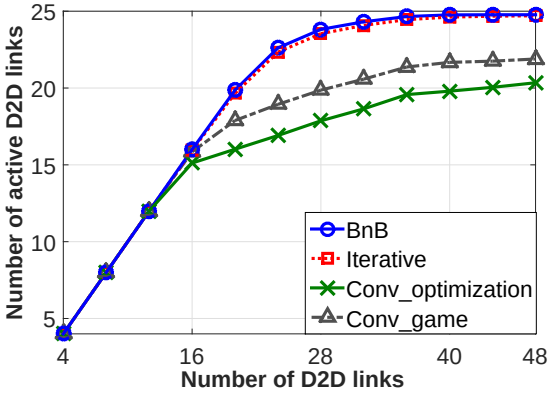

Fig. 12. Number of active D2D links versus K_d as $K_c = 10$

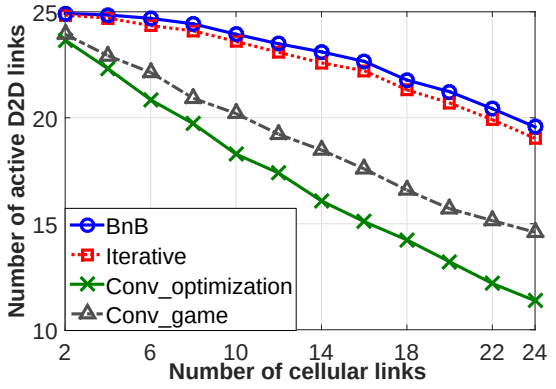

Fig. 10. Number of active D2D links versus K_c as $K_d = 30$

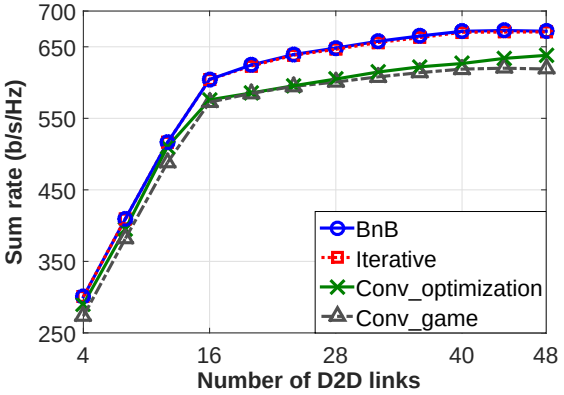

Fig. 11. System sum rate versus K_d as $K_c = 10$

active D2D links decreases, which is confirmed by Fig. 10. Therefore, it results in the decrease of the system sum-rate.

Fig. 11 presents the system sum-rate for varying number of D2D links K_d as we fix $K_c = 10$. It is shown that as K_d increases, the system sum-rate increases quite significantly for all algorithms. In fact, as K_d increases, number of active D2D links increases, which is confirmed by Fig. 12; therefore, the higher number of D2D links K_d leads to the greater system sum-rate. Moreover, since K_c is small, as K_d increases, D2D links can access the large bandwidth, which results in significant improvement of the system sum-rate.

C. Numerical Results for Scenario II

We now study the achievable network performance when the Iterative Rounding Algorithm is utilized to address scenario II where each active D2D link can be assigned multiple subbands. We compare our proposed algorithms with the algorithms in [27] and [28] denoted as "Conventional 1" and "Conventional 2" algorithms. The former algorithm performs resource allocation by using the coalitional game approach where the coalitions are determined by a greedy algorithm. The latter algorithm implements the resource allocation by using merge-and-split coalitional game method.

Results for all proposed algorithms presented in the following employ the Iterative Rounding algorithm, and they are different in the methods employed to determine the number of subbands assigned to each D2D link in step one of the proposed two-step approach. While in the "Proposed single" algorithm, each D2D link is assigned one subband, the "Proposed Extension 1" and "Proposed Extension 2" determine the number of subbands assigned to each D2D link by using the outcomes of "Conventional 1" and "Conventional 2" algorithms, respectively. Moreover, the "Proposed multi-fair" algorithm assigns the same number of subbands to all admitted D2D links. We also consider the "Full admission" scheme where all D2D links are admitted without performing adaptive D2D link selection. Finally, the "Proposed multi-sequential" algorithm determines the number of subbands for D2D links as follows. First, each D2D link is assigned one subband. Then, if there are still available subbands, we sequentially assign one more subband to one D2D link, which results in the highest improvement of the system sum-rate in each iteration.

Figs. 13 and 14 show the sum-rate versus the number of cellular links K_c as $K_d = 25$ (K_d is shown, otherwise). It can be seen that the proposed algorithms ("Proposed single", "Proposed Extension 1", and "Proposed Extension 2") perform significantly better than the conventional algorithms, which confirms the efficacy of the proposed joint subband and power allocation design. The "Proposed single" algorithm even performs better than the "Proposed Extension 1" and "Proposed Extension 2" algorithms. This implies that in the dense D2D communication scenario, assignment of a single subband for each D2D link results in sufficiently good performance. In

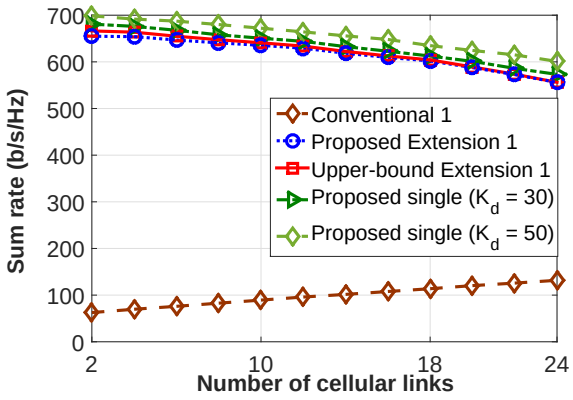

Fig. 13. Sum rate versus K_c (Comparing with [27])

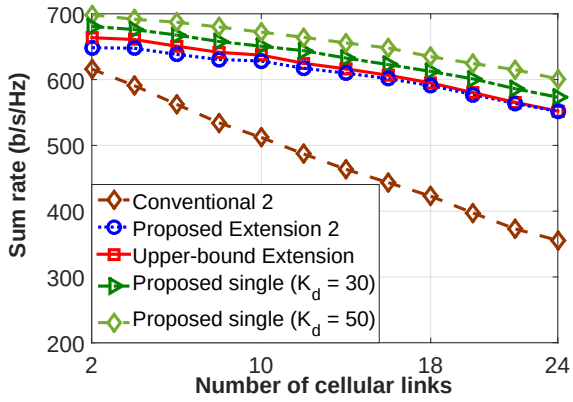

Fig. 14. Sum rate versus K_c (Comparing with [28])

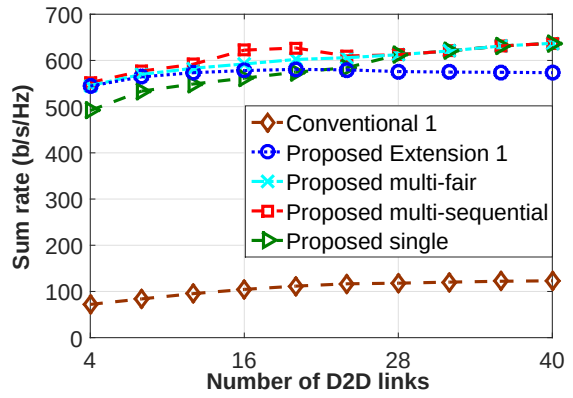

Fig. 15. Sum rate versus K_d (Comparing with [27])

addition, the "Proposed single" algorithm achieves higher sum rate for $K_d = 50$ than for $K_d = 25$ thanks to the additional multiuser diversity gain. Finally, the "Proposed single" algorithm results in better sum-rate than that of the "Full admission", which demonstrates the benefits of adaptive D2D link selection.

Figs. 15 and 16 show the sum-rate versus the number of D2D links K_d as $K_c = 20$. It is shown that as K_d is small, assignment of multiple subbands for each D2D link (scenario II) can result in better performance. However, as the number of D2D links increases, the performance gap among different designs for scenarios I and II decreases.

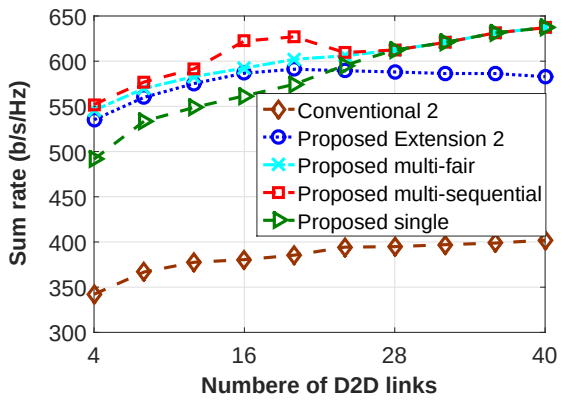

Fig. 16. Sum rate versus K_d (Comparing with [28])

Moreover, except for cases where K_d is in the interval [8, 16], the performances of the "Proposed multi-fair" and "Proposed multi-sequential" algorithms are similar. This illustrates the regions where fair subband allocation can be adopted to enjoy both low computation complexity and good performance.

VII. Conclusion

In this paper, we have developed efficient resource allocation algorithms for D2D underlaid cellular network systems. The proposed algorithms are differentiated mainly by their subband assignment designs, which are developed based on the optimal power allocation solution for individual pairs of cellular and D2D links on any subband. We have established the theoretical performance guarantee for the Iterative Rounding algorithm and analyzed the computational complexity of the proposed algorithms. Numerical results have confirmed that the proposed designs result in better performance than state-of-the-art algorithms.

Appendix A
Proof of Proposition 1

In problem (14), we only consider subband n. Therefore, we omit the index n in this Appendix for brevity. If the optimal power of problem (14) belongs to the set $(P_k^{\max}, p_{Dl})$, then we only have to find the optimal power allocation of D2D link i.e., p_{Dl}. The rates achieved by cellular link k and D2D link l can be expressed, respectively, as $r_{Ck} = \log_2\left(1 + P_k^{\max} h_{kk}/(\sigma_k + p_{Dl} h_{kl})\right)$, and $r_{Dl} = \log_2\left(1 + p_{Dl} h_{ll}/(\sigma_l + P_k^{\max} h_{lk})\right)$.

It can be verified that r_{Ck} is monotonically decreasing with p_{Dl}; hence, to satisfy minimum rate requirement of cellular link k we must have $p_{Dl} \leq \left(P_k^{\max} h_{kk}/(2^{R_k^{\min}} - 1) - \sigma_k\right)/h_{kl}$. Similarly, r_{Dl} is monotonically increasing with p_{Dl}. Hence, $p_{Dl} \geq (2^{R_l^{\min}} - 1)(P_k^{\max} h_{lk} + \sigma_l)/h_{ll}$. As a result, to obtain a feasible solution, we must have $p_{Dl} \in [P_{Dl}^{(1)}, P_{Dl}^{(2)}]$, where

$$P_{Dl}^{(1)} = \max\left\{\frac{(2^{R_l^{\min}} - 1)(P_k^{\max} h_{lk} + \sigma_l)}{h_{ll}},\ 0\right\} \tag{34}$$

$$P_{Dl}^{(2)} = \min\left\{\frac{1}{h_{kl}}\left(\frac{P_k^{\max} h_{kk}}{2^{R_k^{\min}} - 1} - \sigma_k\right),\ P_l^{\max}\right\}. \tag{35}$$

In addition, we modify w_{kl} as $w_{kl} = \alpha(r_{Ck} + \beta r_{Dl})$ where $\beta = (1-\alpha)/\alpha$. Now we define

$$f(p_{Dl}) = \left(1 + \frac{P_k^{\max} h_{kk}}{\sigma_k + p_{Dl} h_{kl}}\right)\left(1 + \frac{p_{Dl} h_{ll}}{\sigma_l + P_k^{\max} h_{lk}}\right)^{\beta}. \quad (36)$$

Then, maximizing w_{kl} is *equivalent to* maximizing $f(p_{Dl})$. The optimal value of $f(p_{Dl})$ can be found by solving the equation $f'(p_{Dl}) = 0$. The derivative of $f(p_{Dl})$ can be expressed as $f'(p_{Dl}) = (A_{Dl} p_{Dl}^2 + 2B_{Dl} p_{Dl} + C_{Dl})/D_{Dl}$ where $A_{Dl} = \beta h_{ll} h_{kl}^2$, $B_{Dl} = 0.5(\beta - 1) P_k^{\max} h_{kk} h_{kl} h_{ll} + \beta \sigma_k h_{kl} h_{ll}$, $C_{Dl} = \beta \sigma_k h_{ll}(\sigma_k + P_k^{\max} h_{kk}) - P_k^{\max} h_{kk} h_{kl}(\sigma_l + P_k^{\max} h_{lk})$, and $D_{Dl} = (\sigma_l + P_k^{\max} h_{lk})(\sigma_k + p_l h_{kl})^2$.

If $\triangle_{Dl} = B_{Dl}^2 - A_{Dl} C_{Dl} > 0$, $f'(p_{Dl}) = 0$ has two solutions $(-B_{Dl} \pm \sqrt{\triangle_{Dl}})/A_{Dl}$. In addition, $(-B_{Dl} - \sqrt{\triangle_{Dl}})/A_{Dl} < 0$ and $(-B_{Dl} + \sqrt{\triangle_{Dl}})/A_{Dl}$ are respectively the minimum and maximum points of function $f(p_{Dl})$. Let us denote $P_{Dl}^{(3)} = (-B_{Dl} + \sqrt{\triangle_{Dl}})/A_{Dl}$. If $P_{Dl}^{(3)} \in [P_{Dl}^{(1)}, P_{Dl}^{(2)}]$, $P_{Dl}^{(3)}$ is the optimal solution of problem (14). On the other hand, if $P_{Dl}^{(3)} \notin [P_{Dl}^{(1)}, P_{Dl}^{(2)}]$, $f(p_{Dl})$ is a monotonic function in $[P_{Dl}^{(1)}, P_{Dl}^{(2)}]$; therefore, $P_{Dl}^{(1)}$ or $P_{Dl}^{(2)}$ is the optimal solution of problem (14).

If $\triangle_{Dl} < 0$, which means that $f'(p_{Dl}) > 0 \ \forall p_{Dl}$ or $f(p_{Dl})$ is a monotonic function of p_{Dl} then $f(p_{Dl})$ achieves its maximum at $P_{Dl}^{(1)}$ or $P_{Dl}^{(2)}$. Therefore, in any cases, the optimal solution of problem (14) belongs to $\mathcal{S}_1$ which completes the proof of the proposition.

Appendix B
Proof of Proposition 3

We prove the proposition by contradiction. Specifically, we show that if $\mathbf{x}_u^*$ is not an optimal solution of problem $\mathbf{LP}(V_u^{(t)}, E(V_u^{(t)}))$, then $\mathbf{x}^*$ is not the optimal solution of problem $\mathbf{LP}(V^{(t)}, E^{(t)})$. First, consider problem $\mathbf{LP}(V, E)$ and let us denote $l(V, E, \mathbf{x})$ as the objective value associated with $\mathbf{x}$ and the optimal objective value is $l^*(V, E)$. Suppose that $\mathbf{x}^o \neq \mathbf{x}_u^*$ is the optimal solution of problem $\mathbf{LP}(V_u^{(t)}, E(V_u^{(t)}))$. Now we define a new vector $\mathbf{x}'$ where the value of its element is set as $x'_e = 1$ if $e \in E_a^{(t)}$, $x'_e = x_e^o$ if $e \in E(V_u^{(t)})$, and $x'_e = 0$, otherwise. On the other hand, we have

$$l(V^{(t)}, E^{(t)}), \mathbf{x}^*) = l(V_a^{(t)}, E(V_a^{(t)}), \mathbf{x}_a^*) + l(V_u^{(t)}, E(V_u^{(t)}), \mathbf{x}_u^*) \quad (37)$$

$$l(V^{(t)}, E^{(t)}), \mathbf{x}') = l(V_a^{(t)}, E(V_a^{(t)}), \mathbf{x}_a^*) + l(V_u^{(t)}, E(V_u^{(t)}), \mathbf{x}^o). \quad (38)$$

Since $l(V_u^{(t)}, E(V_u^{(t)}), \mathbf{x}_u^*) < l(V_u^{(t)}, E(V_u^{(t)}), \mathbf{x}^o)$, we have $l(V^{(t)}, E^{(t)}, \mathbf{x}^*) < l(V^{(t)}, E^{(t)}, \mathbf{x}')$. Hence, $\mathbf{x}^*$ is not the optimal solution of $\mathbf{LP}(V^{(t)}, E^{(t)})$, which is a contradiction.

Appendix C
Proof of proposition 4

The proof of Proposition 4 is equivalent to the proof of the following inequality

$$\sum_{e \in E_s^{(1)}} w_e \geq \frac{1}{2} \sum_{e \in E_u^{(t)}} x_e^* w_e, \quad (39)$$

where $E_s^{(1)}$ is the set of edges returned in Algorithm $\mathbf{LR}(E_u^{(t)}, \mathbf{w}(E_u^{(t)}))$, and x_e^* corresponds to edge e in $\mathbf{x}_u^*$ which is the optimal solution of problem $\mathbf{LP}(V_u^{(t)}, E(V_u^{(t)}))$. To complete the proof of this proposition, we use the results in the following lemma whose proof can be adapted from that in [38] with some minor modifications.

Lemma 1. *In iteration t of Algorithm 1, the chosen edge e^* in each sub-iteration i always has the coupling parameter with the unarranged edges ($E_{uu}^{(t)}$) being smaller than 2, i.e.., $c(e^*, E_{uu}^{(t)}) \leq 2$.*

Recall that we employ the *Local Ratio Method* in Algorithm 2 to allocate the resources to some fractional edges in $E_u^{(t)}$. Therefore, all the lines mentioned in the following correspond to Algorithm 2. We notice that each time we update E_{temp} (line 5), we also modify weighted vector of $E_u^{(t)}$ (line 6). Therefore, we have $|E_{\mathsf{temp}}| + 1$ iterations updating the weight vector of $E_u^{(t)}$. We define $\mathbf{w}^{(j)}(E_u^{(t)})$ and $\bar{\mathbf{w}}^{(j)}(E_u^{(t)})$ respectively as the weight vectors of $E_u^{(t)}$ before and after weight update in iteration j ($1 \leq j \leq |E_{\mathsf{temp}}| + 1$). We now define $\hat{\mathbf{w}}^{(j)}(E_u^{(t)}) = \mathbf{w}^{(j)}(E_u^{(t)}) - \bar{\mathbf{w}}^{(j)}(E_u^{(t)})$. In addition, we denote $w_e^{(j)}$, $\bar{w}_e^{(j)}$, and $\hat{w}_e^{(j)}$ are respectively the elements corresponding to edge e in $\mathbf{w}_e^{(j)}$, $\bar{\mathbf{w}}_e^{(j)}$, and $\hat{\mathbf{w}}_e^{(j)}$. Note that in lines 3 and 10 in Algorithm 2 we consider the same set of edges E_{temp}; therefore, each index j ($1 \leq j \leq |E_{\mathsf{temp}}|$) in lines 3 and 10 corresponds to a specific edge $e_j \in E_{\mathsf{temp}}$.

We prove the proposition by induction on number of edges in $E_s^{(j)}$. At first, the statement in the proposition holds in the base case at iteration $j = |E_{\mathsf{temp}}| + 1$ since at that iteration $E_s^{(|E_{\mathsf{temp}}|+1)} = \emptyset$ and $\mathbf{w}^{(|E_{\mathsf{temp}}|+1)}(E_u^{(t)}) \leq \mathbf{0}$, where $\mathbf{0}$ is a zero vector. We assume the induction hypothesis that at any iteration j ($1 < j \leq |E_{\mathsf{temp}}| + 1$) we have

$$\sum_{e \in E_s^{(j)}} w_e^{(j)} \geq \frac{1}{2} \sum_{e \in E_u^{(t)}} x_e^* w_e^{(j)}. \quad (40)$$

We need to prove the following

$$\sum_{e \in E_s^{(j-1)}} w_e^{(j-1)} \geq \frac{1}{2} \sum_{e \in E_u^{(t)}} x_e^* w_e^{(j-1)}. \quad (41)$$

We assume that at iteration $j-1$ edge e^* is chosen (line 4 or 10). From the edge selection procedure in lines 9-11, we have

$$E_s^{(j-1)} = \begin{cases} E_s^{(j)} & \text{if } e^* \notin E_s^{(j-1)} \\ E_s^{(j)} \cup \{e^*\} & \text{if } e^* \in E_s^{(j-1)}. \end{cases} \quad (42)$$

Due to the employed update procedure for the weight vector, we have $\mathbf{w}^{(j)}(E_u^{(t)}) = \bar{\mathbf{w}}^{(j-1)}(E_u^{(t)})$ and $\bar{w}_{e^*}^{(j-1)} = 0$. Combining these arguments with (42) we have

$$\begin{aligned} \sum_{e \in E_s^{(j-1)}} \bar{w}_e^{(j-1)} &= \sum_{e \in E_s^{(j)}} w_e^{(j)} \\ \sum_{e \in E_u^{(t)}} x_e^* w_e^{(j)} &= \sum_{e \in E_u^{(t)}} x_e^* \bar{w}_e^{(j-1)}. \end{aligned} \quad (43)$$

Using the results in (40) and (43), we arrive at

$$\sum_{e \in E_s^{(j-1)}} \bar{w}_e^{(j-1)} \geq \frac{1}{2} \sum_{e \in E_u^{(t)}} x_e^* \bar{w}_e^{(j-1)}. \quad (44)$$

Assume that E_c is the set of edges coupled with the considered edge e^* in line 6. In addition, each element of $\hat{\mathbf{w}}^{(j-1)}(E_u^{(t)})$ satisfies

$$\hat{w}_e^{(j-1)} = \begin{cases} w_{e^*}^{(j-1)} & \forall e \in E_c \\ 0 & \text{otherwise.} \end{cases} \quad (45)$$

According to Lemma 1, we have $c(e^*, E_c) = \sum_{e \in E_c} x_e^* \leq 2$. Using this result and (45), we obtain

$$\sum_{e \in E_u^{(t)}} x_e^* \hat{w}_e^{(j-1)} \leq 2 w_{e^*}^{(j-1)}. \quad (46)$$

In addition, according to the proposed edge selection procedure (line 10), at least one edge coupled with e^* must belong to $E_s^{(j-1)}$. Therefore,

$$\sum_{e \in E_s^{(j-1)}} \hat{w}_e^{(j-1)} \geq w_{e^*}^{(j-1)}. \quad (47)$$

From (46) and (47), the following inequality holds

$$\sum_{e \in E_s^{(j-1)}} \hat{w}_e^{(j-1)} \geq \frac{1}{2} \sum_{e \in E_u^{(t)}} x_e^* \hat{w}_e^{(j-1)}. \quad (48)$$

Combining the fact that $\mathbf{w}^{(j-1)}(E_u^{(t)}) = \bar{\mathbf{w}}^{(j-1)}(E_u^{(t)}) + \hat{\mathbf{w}}^{(j-1)}(E_u^{(t)})$ and the results from (44) and (48), we have

$$\sum_{e \in E_s^{(j-1)}} w_e^{(j-1)} \geq \frac{1}{2} \sum_{e \in E_u^{(t)}} x_e^* w_e^{(j-1)}, \quad (49)$$

which complies with (41) . On the other hand, as $j = 1$, we have $\mathbf{w}(E_u^{(t)}) = \mathbf{w}^{(1)}(E_u^{(t)})$; therefore, the inequality (39) holds.

APPENDIX D
PROOF OF PROPOSITION 5

To address the considered subband assignment problem, we have reformulated an equivalent problem $\mathbf{IP}(V^0, E^0)$ where we have created $(N - K_c)$ cellular virtual links and the degree of each cellular virtual links is smaller than 1. Under this construction, there are at most $(N - K_c)$ D2D links, each of which can use a subband exclusively. Therefore, we can always guarantee that each of K_c cellular links is assigned one subband, which enables them to maintain the minimum rate constraints. In addition, after the first iteration of Algorithm 1, we admit $E_a^{(1)} \cup E_g^{(1)}$. In addition, we have (i): $z(E_a^{(1)} \cup E_g^{(1)}) = z(E_a^{(1)}) + z(E_g^{(1)})$. According to Proposition 3, we arrive at (ii): $l^*(V^{(1)}, E^{(1)}) = l^*(V_u^{(1)}, E(V_u^{(1)})) + z(E_a^{(1)})$. Also Proposition 4 suggests that (iii): $z(E_g^{(1)}) \geq \frac{1}{2} l^*(V_u^{(1)}, E(V_u^{(1)}))$. Combining (i), (ii), and (iii), we have

$$z(E_a^{(1)} \cup E_g^{(1)}) \geq \frac{1}{2} l^*(V^{(1)}, E^{(1)}) = \frac{1}{2} l^*(V^0, E^0). \quad (50)$$

Note that $E_a^{(1)} \cup E_g^{(1)} \subset E_{al}^f$ where E_{al}^f is the set E_{al} obtained at the end of Algorithm 1. Therefore, we have $z(E_{al}^f) \geq \frac{1}{2} l^*(V^0, E^0)$, which finishes the proof of the proposition.

REFERENCES

[1] Ericson, "5G radio access - research and vision," *White paper*, 2013.

[2] X. Lin, J. G. Andrews, A. Ghosh, and R. Ratasuk, "An overview on 3GPP device-to-device proximity services," *IEEE Commun. Mag.*, vol. 52, no. 4, pp. 40–48, Apr. 2014.

[3] T. D. Hoang, L. B. Le, and T. Le-Ngoc, "Energy-efficient resource allocation for D2D communications in cellular networks," *IEEE Trans. on Veh. Tech.*, 2015, to be published.

[4] T. D. Hoang, L. B. Le, and T. Le-Ngoc, "Dual decomposition method for energy-efficient resource allocation in D2D communications underlying cellular networks," *in Proc. IEEE Globecom'2015*, Dec. 2015.

[5] 3GPP, "3rd generation partnership project; technical specification group services and system aspects; service requirements for the Evolved Packet System (EPS) (Release 13)," *TS 22.278 V13.2.0*, Dec. 2014.

[6] Z.-Q. Luo and S. Zhang, "Dynamic spectrum management: Complexity and duality," *IEEE J. Sel. Topics Signal Process.*, vol. 2, no. 1, pp. 57–73, Feb. 2008.

[7] C. H. Yu, K. Doppler, C. B. Ribeiro, and O. Tirkkonen, "Resource sharing optimization for device-to-device communication underlaying cellular networks," *IEEE Trans. Wireless Commun.*, vol. 10, no. 8, pp. 2752–2763, Aug. 2011.

[8] H. Song, J. Y. Ryu, W. Choi, and R. Schober, "Joint power and rate control for Device-to-Device communications in cellular systems," *IEEE Trans. Wireless Commun.*, vol. 14, no. 10, pp. 5750–5762, Oct. 2015.

[9] D. Feng, G. Yu, C. Xiong, Y. Yuan-Wu, G. Y. Li, G. Feng, and S. Li, "Mode Switching for energy-efficient Device-to-Device communications in cellular networks," *IEEE Trans. Wireless Commun.*, vol. 14, no. 12, pp. 6993–7003, Dec. 2015.

[10] M. Azam, M. Ahamad, M. Naeem, M. Iqbal, A. S. Khwaja, A. Anpalagan, and S. Quaser, "Joint admission control, mode selection and power allocation in D2D communication systems," *IEEE Trans. Veh. Tech.*, 2015, to be published.

[11] D. Feng, L. Lu, Y. W. Yi, G. Y. Li, G. Geng, and S. Li, "Device-to-device communications underlaying cellular networks," *IEEE Trans. Commun.*, vol. 61, no. 8, pp. 3541–3551, Aug. 2013.

[12] G. Yu, L. Xu, D. Feng, R. Yin, G. Y. Li, and Y. Jiang, "Joint mode selection and resource allocation for Device-to-Device communications," *IEEE Trans. Commun.*, vol. 62, no. 11, pp. 3814–3824, Nov. 2014.

[13] X. Ma, J. Liu, and H. Jiang, "Resource allocation for heterogeneous applications with D2D communication underlaying cellular networks," *IEEE J. Sel. Areas Commun.*, vol. 34, no. 1, pp. 15–26, Jan. 2016.

[14] Y. Gu, Y. Zhang, M. Pan, and Z. Han, "Matching and cheating in Device to Device communications underlying cellular networks," *IEEE J. Sel. Areas Commun.*, vol. 33, no. 10, pp.2156–2166, Oct. 2015.

[15] L. Wang and G. L. Stuber, "Pairing for resource sharing in cellular Device-to-Device underlays," *IEEE Network*, vol. 30, no. 2, pp. 122 –128, Mar. 2016.

[16] Y. Ren, F. Liu, Z. Liu, C. Wang, and Y. Ji, "Power control in D2D-based vehicular communication networks," *IEEE Trans. Veh. Tech.*, vol. 64, no. 12, pp. 5547–5562, Dec. 2015.

[17] L. A.-Kanj, H. V. Poor, and Z. Dawy, "Optimal cellular offloading via D2D Communication networks with fairness constraints," *IEEE Trans. Wireless Commun.* vol. 13, no. 8, pp. 4628–4643, Aug. 2014.

[18] F. Malandrino, Z. Limani, C. Casetti, and C. F. Chiasserini, "Interference-aware downlink and uplink resource allocation in Hetnets with D2D support," *IEEE Trans. Wireless Commun.*, vol. 14, no. 5, pp. 2729–2741, Jan. 2015.

[19] S. Maghsudi and S. Stanczak, "Hybrid centralized-distributed resource allocation for Device-to-Device communication underlaying cellular networks," *IEEE Trans. Veh. Tech.*, vol. 65, no. 4, pp. 2481–2495, Apr. 2016.

[20] R. Yin, C. Zhong, G. Yu, Z. Zhang, K. K. Wong, and X. Chen, "Joint spectrum and power allocation for D2D communications underlaying cellular networks," *IEEE Trans. Veh. Tech.*, vol. 65, no. 4, pp. 2182–2195, Apr. 2016.

[21] W. Zhao and S. Wang, "Resource sharing scheme for Device-to-Device communication underlaying cellular networks," *IEEE Trans. Commun.*, vol. 63, no. 12, pp. 4838–4848, Dec. 2015.

[22] H. Zhang, L. Song, and Z. Han, "Radio resource allocation for Device-to-Device underlay communication using hypergraph theory," *IEEE Trans. Wireless Commun.*, vol. 15, no. 7, pp. 4852–4861, July 2016.

[23] R. Zhang, X. Cheng, L. Yang, and B. Jiao, "Interference graph based resource allocation (InGRA) for D2D Communications underlaying cellular networks," *IEEE Trans. Veh. Technol.*, vol. 64, no. 8, pp. 3844–3850, Aug. 2015.

[24] C. Xu, L. Song, Z. Han, Q. Zhao, X. Wang, X. Cheng, and B. Jiao, "Efficiency resource allocation for device-to-device underlay communication systems: A reverse iterative combinatorial auction based approach," *IEEE J. Sel. Areas Commun.*, vol. 31, no. 9, pp. 348–358, Sep. 2013.
[25] Q. Ye, M. Al-Shalash, C. Caramanis, and J. G. Andrews, "Distributed resource allocation in device-to-device enhanced cellular networks," *IEEE Trans. Commun.*, vol. 63, no. 2, pp. 441–454, Feb. 2015.
[26] R. Yin, G. Yu, H. Zhang, Z. Zhang, and G. Y. Li, "Pricing-based interference coordination for D2D communications in cellular networks," *IEEE Trans. Wireless Commun.* vol. 14, no. 3, pp. 1519–1532, Mar. 2015.
[27] D. Wu, J. Wang, R. Q. Hu, Y. Cai, and L. Zhou, "Energy-efficient resource sharing for mobile Device-to-Device multimedia communications," *IEEE Trans. Veh. Tech.*, vol. 63, no. 5, pp. 2093–2103, Jun. 2014.
[28] D. Wu, Y. Cai, R. Q. Hu, and Y. Qian, "Dynamic distributed resource sharing for mobile D2D communications," *IEEE Trans. Wireless Commun.*, vol. 14, no. 10, pp. 5417–5429, Oct. 2015.
[29] Y. Zhao, Y. Li, Y. Cao, T. Jiang, and N. Ge, "Social-aware resource allocation for Device-to-Device communications underlaying cellular networks," *IEEE Trans. Wireless Commun.*, vol. 14, no. 12, pp. 6621–6634, Dec. 2015.
[30] T. D. Hoang, L. B. Le, and T. Le-Ngoc, "Joint subchannel and power allocation for D2D communications in cellular networks," in *Proc. IEEE WCNC'2014*, Apr. 2014.
[31] T. D. Hoang, L. B. Le, and T. Le-Ngoc, "Resource allocation for D2D communications under proportional fairness," *in Proc. IEEE Globecom'2014*, Dec. 2014.
[32] R. B. Yehuda, K. Bendel, A. Freund, and D. Rawitz, "Local ratio: A unified framework for approximation algorithms. In memorian: Shimon Even 1935–2004," *ACM Comput. Surv.*, vol. 36, no. 4, pp. 422–463, Dec. 2004.
[33] A. Abdelnasser, E. Hossain, and D. I. Kim, "Tier-aware resource allocation in OFDMA macrocell-small cell networks," *IEEE Trans. Commun.*, vol. 63, no. 3, pp. 695–710, Feb. 2015.
[34] M. Ebrahimi, M. A. Maddah-Ali, and A. K. Khandani, "Power allocation and asymptotic achievable sum-rates in single-hop wireless networks, in *Proc. IEEE CISS*, 2006, pp. 498–503, Mar. 2006.
[35] C. Roos, T. Terlaky, and J. Vial, "Interior point methods for linear optimization," *Springer*, Press, 2005.
[36] H. W. Kuhn, "The Hungurian method for the assignment problem, " *Naval Res. Logistics Quart.*, vol. 2, no. 1, pp. 83–97, Mar. 1955.
[37] D. Gale and L.S. Shapley, "College admissions and the stability of marriage," *Amer. Math. Monthly*, vol. 69, no. 1, pp. 9–15, Jan. 1962.
[38] L. C. Lau, R. Ravi, and M. Singh, "Iterative methods in combinatorial optimization," *Cambridge Univ. Press*, 2011.

Tuong Duc Hoang (S'14) received the B.Eng. (Honor) degree from Hanoi University of Technology, Vietnam, in 2010, and the M.S. degree from Korea Advanced Institute of Science and Technology (KAIST), Daejeon, Korea, in 2013. He is currently a Ph.D. candidate at the Institut National de la Recherche Scientifique-Energy, Materials, and Telecommunications Center (INRS-EMT), Université du Québec, Montréal, QC, Canada. His research interest includes radio resource management for wireless communication systems with special emphasis on heterogeneous networks including D2D communications and dense networks.

Long Bao Le (S'04-M'07-SM'12) received the B.Eng. (with Highest Distinction) degree from Ho Chi Minh City University of Technology, Vietnam, in 1999, the M.Eng. degree from Asian Institute of Technology, Pathumthani, Thailand, in 2002, and the Ph.D. degree from the University of Manitoba, Winnipeg, MB, Canada, in 2007. He was a postdoctoral researcher at Massachusetts Institute of Technology (2008-2010) and University of Waterloo (2007-2008). Since 2010, he has been with the Institut National de la Recherche Scientifique (INRS), Université du Québec, Montréal, QC, Canada where he is currently an associate professor. His current research interests include smartgrids, cognitive radio and dynamic spectrum sharing, radio resource management, network control and optimization for wireless networks. He is a co-author of the book *Radio Resource Management in Multi-Tier Cellular Wireless Networks* (Wiley, 2013). Dr. Le is a member of the editorial board of *IEEE Communications Surveys and Tutorials* and *IEEE Wireless Communications Letters*. He has served as a technical program committee chair/co-chair for several IEEE conferences including IEEE WCNC, IEEE VTC, and IEEE PIMRC.

Tho Le-Ngoc (F97) obtained his B.Eng. (with Distinction) in Electrical Engineering in 1976, his M.Eng. in 1978 from McGill University, Montreal, Canada, and his Ph.D. in Digital Communications in 1983 from the University of Ottawa, Canada. During 1977-1982, he was a R&D Senior Engineer with Spar Aerospace Limited, Ste. Anne-de-Bellevue, Canada, and involved in the development and design of satellite communications systems. During 1982-1985, he was Engineering Manager of the Radio Group in the Department of Development Engineering of SRTelecom Inc., St. Laurent, Canada, where he developed the new point-to-multipoint DA-TDMA/TDM Subscriber Radio System SR500. During 1985-2000, he was a Professor at the Department of Electrical and Computer Engineering of Concordia University, Montreal, Canada. Since 2000, he has been with the Department of Electrical and Computer Engineering of McGill University. His research interest is in the area of broadband digital communications. He is a fellow of the Institute of Electrical and Electronics Engineers (IEEE), the Engineering Institute of Canada (EIC), the Canadian Academy of Engineering (CAE) and the Royal Society of Canada (RSC). He is the recipient of the 2004 Canadian Award in Telecommunications Research, and recipient of the IEEE Canada Fessenden Award 2005. He holds a Canada Research Chair (Tier I) on Broadband Access Communications.